AFCRL-62-662

THE UNIVERSITY OF MICHIGAN

COLLEGE OF ENGINEERING
Department of Aeronautical and Astronautical Engineering
High Altitude Engineering Laboratory

Final Report

FALLING-SPHERE EXPERIMENT FOR UPPER-AIR-DENSITY: INSTRUMENTATION DEVELOPMENTS

Prepared for the Project by:

H. F. Schulte
D. A. Robinson
J. L. Wagener

Approved by:

L. M. Jones

Project 6690
Task 66900

ORA Project 03558

under contract with:

UNITED STATES AIR FORCE
OFFICE OF AEROSPACE RESEARCH
GEOPHYSICS RESEARCH DIRECTORATE
L. G. HANSCOM FIELD
BEDFORD, MASSACHUSETTS
CONTRACT NO. AF 19(604)-6185

administered through:

OFFICE OF RESEARCH ADMINISTRATION ANN ARBOR

April 1962

TABLE OF CONTENTS

LIST OF TABLES

LIST OF FIGURES

LIST OF FIGURES (Concluded)

ABSTRACT

The continuing development of the instrumentation for the falling-sphere experiment for upper-air density and temperature is described. A multiple-circuit cavity for the accelerometer, which permitted the elimination of the wire bobbin contact, was developed. A moving iron solenoid caging device resulted in a smaller accelerometer requiring less power than the previous model. A new Attwood's machine permitting laboratory tests at 10^{-3} g was constructed. Electronic circuits were developed to replace the intervalometer motor. Circuits were also devised to permit long transit times and to provide discrimination between start and stop pulses. Four spheres and accelerometers for flight test were constructed.

THE UNIVERSITY OF MICHIGAN PROJECT PERSONNEL

(Both Full Time and Part Time)

Estry, Hal W., B.S., Assistant Research Engineer
Filsinger, Edward A., Instrument Maker
Gleason, Kermit L., Instrument Maker
Jones, Leslie M., B.S., Laboratory Director
Mosakewicz, Mary C., Secretary
Peterson, John W., M.S., Associate Research Engineer
Robinson, Douglas A., Technician
Schulte, Hal F., Jr., M.S., Associate Research Engineer
Sporzynski, George A., B.S., Technician
Wagener, Jerrold L., B.S., Assistant Research Engineer
Work, Edgar A., B.S., Assistant Research Engineer

I. INTRODUCTION

This is the final report of a project carried on in the Department of Aeronautical and Astronautical Engineering of The University of Michigan, the purpose of which was to complete certain developments of the falling-sphere method for measuring upper-air density and temperature. The immediate predecessor of this contract was Contract No. AF 19(604)-2415 under which the developments reported herein were initiated. For a report of the preliminary work, see University of Michigan Engineering Research Institute Report 2649-9-F. The sphere development program of the current contract is a continuation of experimental work with small spheres started in 1954. Background information is contained in Refs. 1 through 9.

The tasks of the contract were as follows:

"Item 1: Develop, construct and test three (3) each completely operational transit-time accelerometers of improved design for use in 7" Falling Sphere experiment. The following improvements in the new design shall be attempted:

"a. Improved release and pick-up mechanism that eliminates, or reduces to an acceptable minimum, the error due to initial velocity of the bobbin.

"b. A more positive and less fragile detection system for determining the bobbin time of flight.

"c. An increase in overall sensitivity and accuracy over the present accelerometer version.

"d. Positive alignment techniques, where possible, to facilitate static and dynamic balance.

"e. Lighter construction, where feasible, to reduce the mass.

"f. Power drain as low as engineering expediency will permit.

"g. Compatibility for use with power transistors currently available.

"Item 2: Develop, construct and test 7" sphere electronic instrumentation compatible with new accelerometer.

"Item 3: Fabricate three (3) each operational sphere instrumentations complete with accelerometer(s) and power supplies.

"Item 4: Modify ground-station equipment to provide compatibility with

new instrumentation."

In summary, a new accelerometer was designed and tested in the laboratory. It was smaller and lighter and consumed less power than the previous version. Further, the design successfully dispensed with the "cats-whisker" bobbin contactor. Laboratory tests (including tests on a new Attwood's machine designed and constructed for this development) indicated good performance. Improved sphere balance was achieved with the aid of a static balance machine. Transistorized sphere circuitry was also designed, built, and tested. It incorporated an electronic intervalometer (instead of motor-driven) to operate the accelerometer. It also employed a discretionary caging circuit to permit measuring long transit times and it generated start and stop pulses of different widths to permit pulse discrimination in the playback system. Because the performance of the accelerometer cannot be adequately evaluated in the laboratory, four spheres and accelerometers for flight test were built. Three of these were flown at Wallops Island in the summer of 1961. All three spheres operated successfully. However, because of rocket failures in two cases, the spheres were not subjected to sufficiently low accelerations to evaluate the low limit of measurable acceleration. Data from the third flight are being reduced. The fourth sphere and accelerometer were delivered to G.R.D. in December, 1961.

2. ACCELEROMETER DEVELOPMENTS

2.1 FIRST MULTIPLE-CAVITY MODEL DEVELOPMENTS

In the previous report the concept of a multiple-circuit cavity which would permit detection of bobbin contact without using the "cat's whisker" contactor was described. The model constructed to test this concept met with some initial successes but, because of the complexity of the caging-finger system, it proved difficult to release the bobbin with an acceptably small initial velocity, and this particular model was abandoned. The multiple-circuit cavity, however, was retained and incorporated with improvements, including capacitative detection of impact, in the final design.

2.2 DEVELOPMENT OF FLIGHT MODEL

On the basis of experience with the original accelerometer and the model described in the preceding paragraph, a third design was undertaken which incorporated sufficient improvements to justify flight tests. This model is the one flown at Wallops Island on June 1 and 6 and July 26, 1961.

The new design, shown in Figs. 1 and 2, employs a bobbin and caging-finger combination similar to that in the original accelerometer. The chief advantages

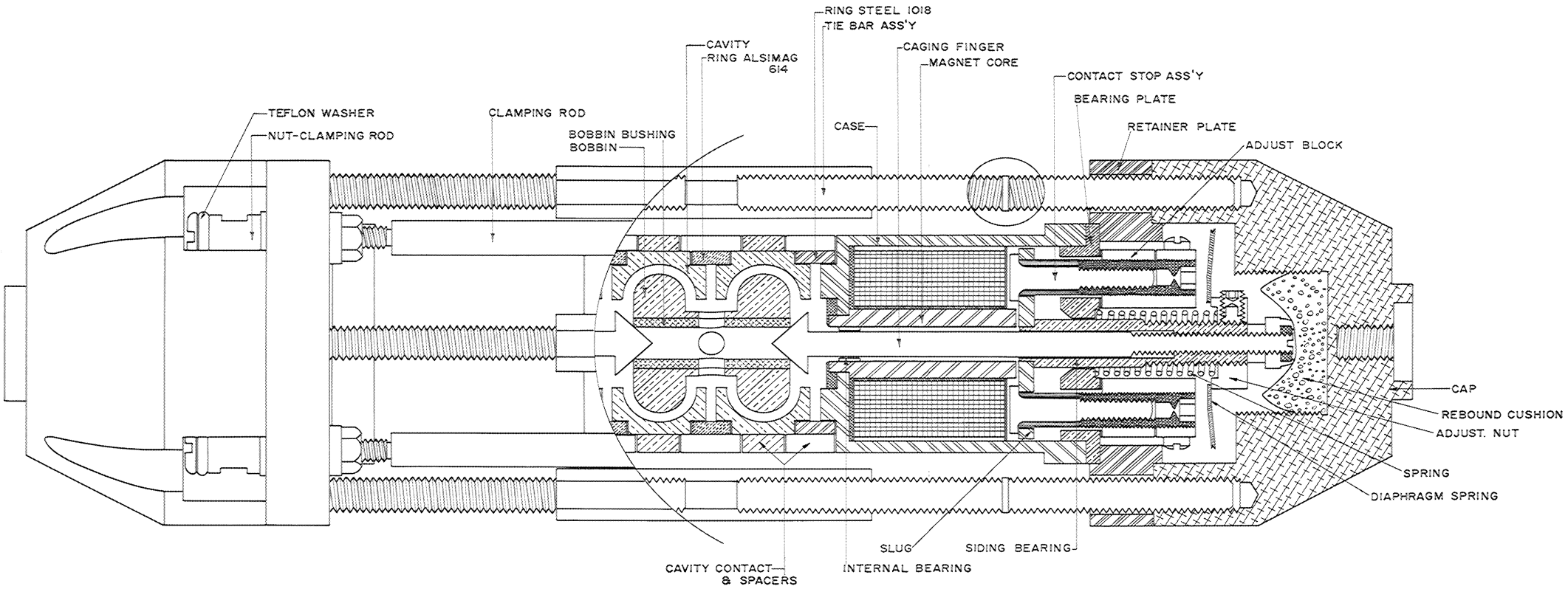

Fig. 1. Assembly drawing of accelerometer.

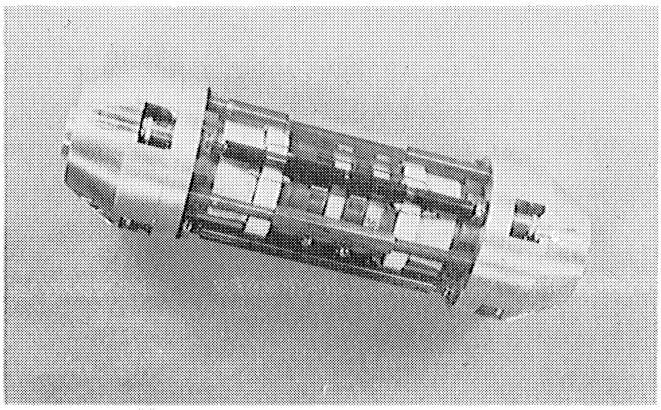

Fig. 2. Photograph of accelerometer.

which affect primarily the initial velocity imparted at release are simplicity and rigidity. Two metal cavity sections surround each lobe of the bobbin through an angle of 180°. The transit distance is 0.050 in. They are separated from each other by an insulating ring. Caging force is provided by two moving iron solenoids on opposite sides of the cavity-bobbin center section. The solenoids are separated from the cavities by rings dimensionally identical to the center ring. One of the cavities is enlarged and is grounded. The ring on that side is of steel. Bobbin release is accomplished by a nonlinear spring system which retracts the caging finger with sufficient speed to escape the pursuing bobbin at 10 g's acceleration. Solenoids were selected for caging because of their relatively small size, low power consumption, and large force exerted in the fully caged position. Disadvantages overcome were: the somewhat greater mass (relative to a moving coil system), a short caging stroke due to rapid diminution of force away from the core, and the presence of residual magnetism.

It was originally thought that tolerances in constructing the various parts could be held close enough so that the bobbin could be used to complete a conductive circuit between the two cavities at any orientation. This proved not to be the case, and we resorted to a capacitive indication of contact between bobbin and cavity. The multiple-circuit cavity was, of course, a necessity for the latter approach so that its conception and development were well used. The capacitive technique eased the very stringent requirements of shop tolerance and in fact allowed actual enlargement (by 0.005 in.) of one cavity so that precision bobbin centering (and thus impact time) was required only at the "close" end of the bobbin and its surrounding cavity. Nevertheless, close tolerances were held in any case to insure an accurate distance in the "close" end, and precision performance in general. Further, although the initial contact time is indeed determined by the "close" end, the wave shape of the contact signal is much more constant with respect to the direction of bobbin travel when one cavity is enlarged.

2.3 CAGING AND RETRACTION

The caging solenoids must pick up the bobbin and various parts of the caging system (depending on orientation) in a 10 g environment. They must also compress the retraction springs. The weights in grams of one set of the moving parts are:

Sliding bearing and slug	11.5
Caging finger	4.4
Adjusting nut	3.5
Coil spring	1.2
Locking nut	0.2
Bobbin	25.0

Given an iron circuit as in Fig. 1, whose dimensions were to some extent dictated by nonrelated design requirements of the sphere and, given a desirable voltage supply of 8 volts d-c, the following coils were found to be best:

wire	No. 26 AWG
turns	680 each coil
resistance	5.2 ohms each coil
current	1.54 amp each coil
ampere turns	1047 each coil
power	24.6 watts total for two coils

The latter figure compares with 54 watts (9 amp at 6 volts) for the original accelerometer. The equilibrium operating temperature of the solenoids was measured as 45.5°C with an iron-constantan thermocouple and Leeds and Northrup potentiometer.

A Hunter force gage Model L-10 was used to measure the retraction force of the caging system. See Fig. 3. Adjustable stops were used to position the slug at various stations of the stroke. The force necessary to pull the slug free from the stops was measured to give a force vs. distance characteristic as seen in Fig. 4. It can be seen that sufficient caging force is available to operate the device over the entire range of displacement, provided that the retracting springs are not too stiff.

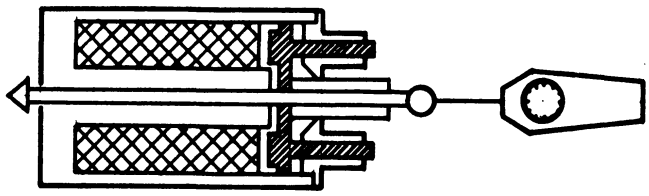

Fig. 3. Set-up for measuring caging force.

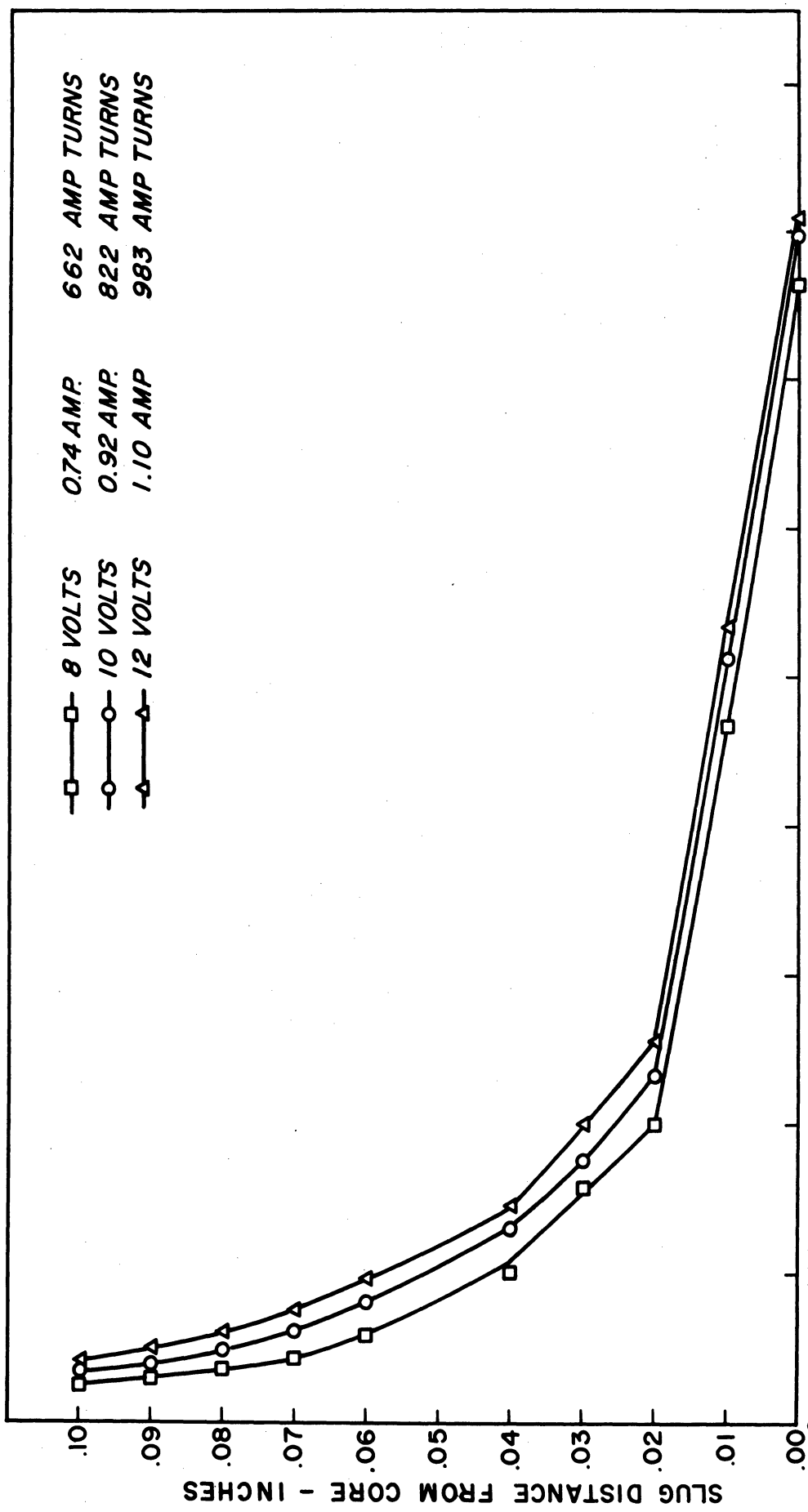

Fig. 4. Caging force vs. displacement.

In the course of choosing the springs it was found necessary and desirable to be able to trace the motion of the caging system. To do this a small vane was attached to the end of the caging finger. The vane intercepted a collimated beam of light directed to a photocell, the output of which was amplified and viewed on an oscilloscope. See Figs. 5 and 6. With this set-up the following significant parameters were measured:

(a) elapsed time for caging and retraction
(b) retraction acceleration
(c) magnitude and duration of rebound
(d) effectiveness of rebound damping
(e) lag time from field collapse to break-free

A variety of springs was tried before deciding on a cascaded combination of two which gave satisfactory initial acceleration together with sustained acceleration. One spring is a helix of ten turns of 0.032-in.-diameter steel wire, the other a flat diaphragm of 0.020-in.-thick beryllium copper. The helical spring operates throughout the entire caging and retraction while the diaphragm is involved in only the last 0.015 in. of the fully caged position. The relatively strong diaphragm was used to achieve the high initial acceleration required by the fingers in the sharp break from the bobbin under 10 g's of acceleration. The acceleration of the caging finger with various spring combinations is shown in Figs. 7, 8, and 9. The displacement of the bobbin under an acceleration of 10 g is shown in each case. Figure 9 is for the combination used in the flight models.

2.2 START SIGNAL

It was at first intended to use the break-free from the stops to generate the start signal, that is, the beginning of the transit time interval. However, the repeated severe hammering of the stops, together with oxidation, caused deterioration of the contact surfaces. Misses in the signal occurred often enough to warrant changing to collapse of the magnetic field as the source of the start signal and then incorporating the constant lag time in the data. The magnitude of the lag time is determined by the residual magnetic field, the distance the slug is stopped from the core, and the forces exerted by the dual spring. The lag time is regulated by varying the deflection of the heavy spring and the positioning of the slug by the adjustable stops. A distance of 0.010 in. between the core and the stops was finally selected after an investigation of the residual magnetic field effects at various distance. This gives control over the too large forces against the core but does not seriously diminish the effective caging distance. Slight changes in this spacing are sometimes made in making the final close balance between the two solenoids. The adjusted lag times in the various accelerometers were about 0.001 second.

The fact that the retraction speed changes under varying acceleration environments is relatively unimportant in the motion of the bobbin as long as the

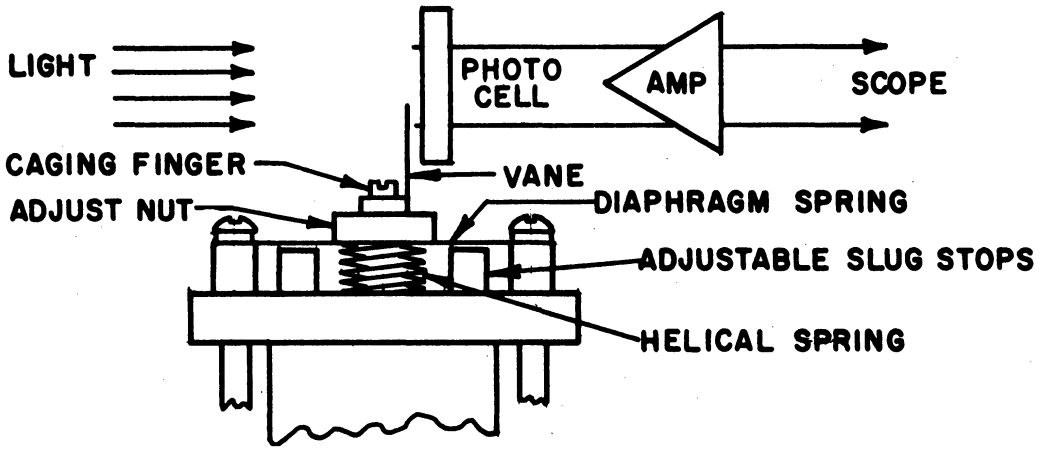

Fig. 5. Vane and photocell for measuring caging finger motion.

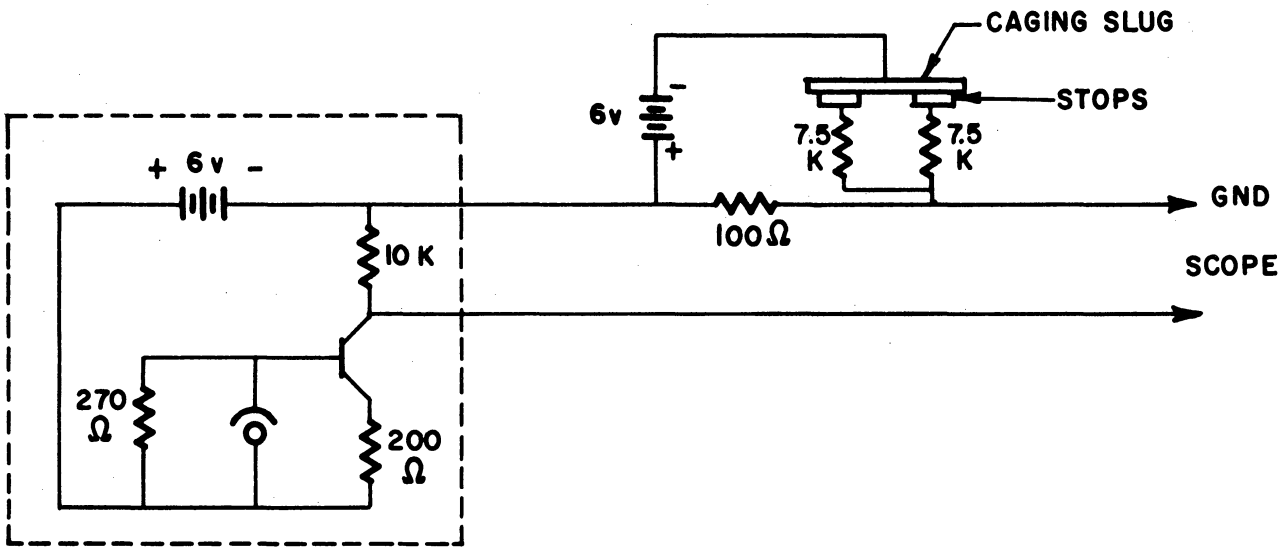

Fig. 6. Transistor amplifer used with vane and photocell.

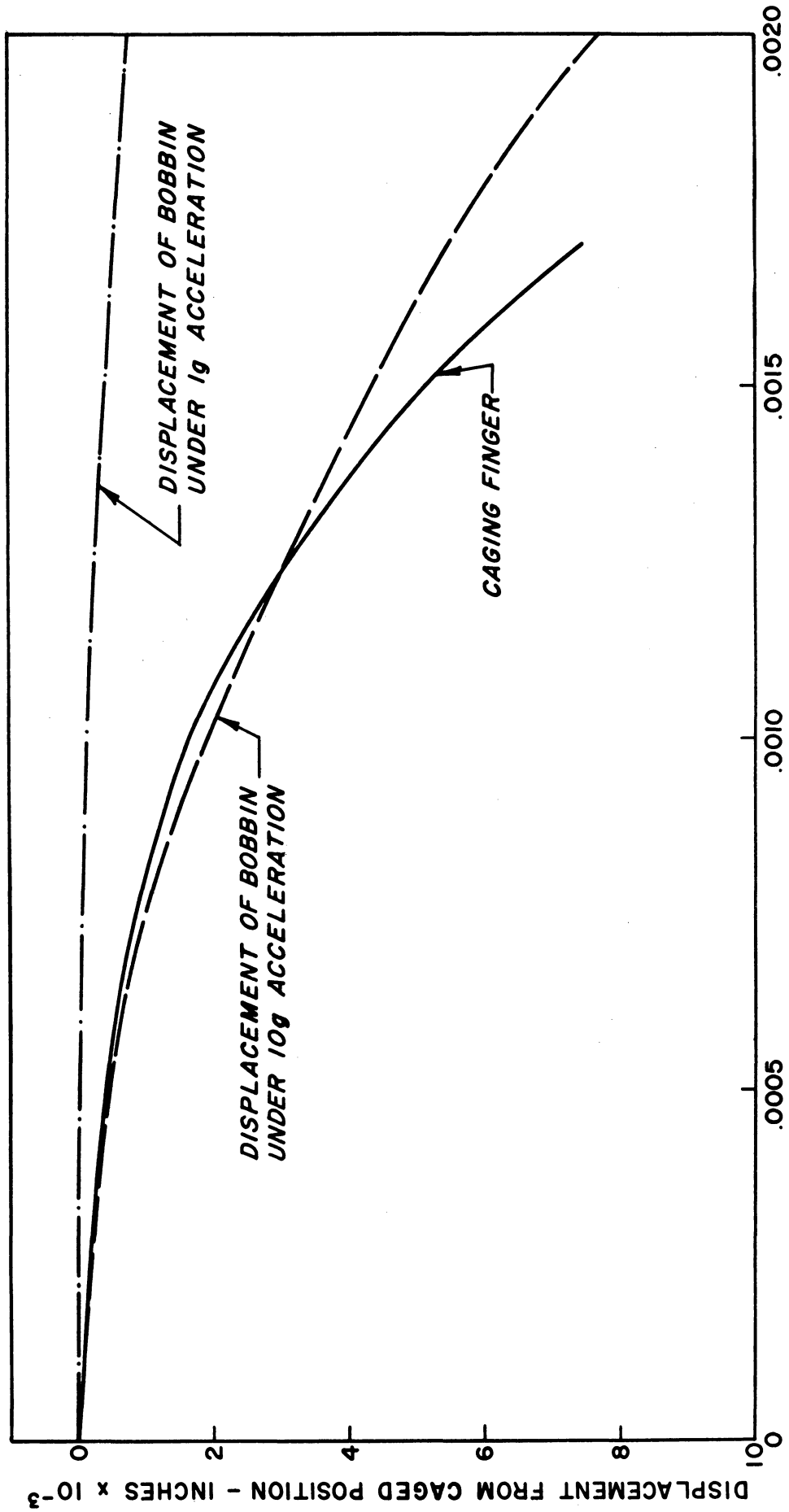

Fig. 7. Caging-finger displacement vs. time. Displacement spring 3, beryllium copper 0.010 in. thick.

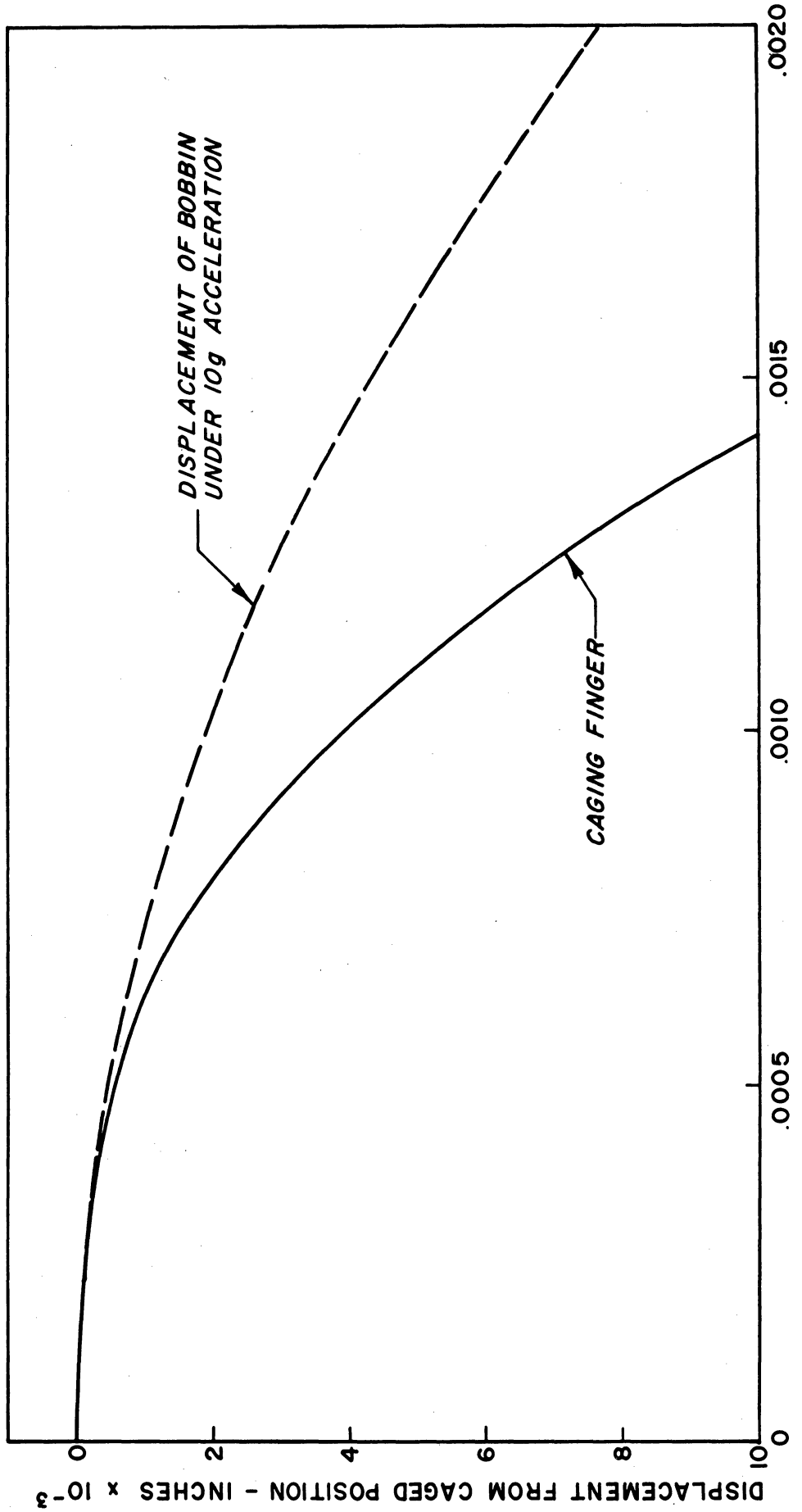

Fig. 8. Caging-finger displacement vs. time. Displacement spring 7, beryllium copper 0.015 in. thick.

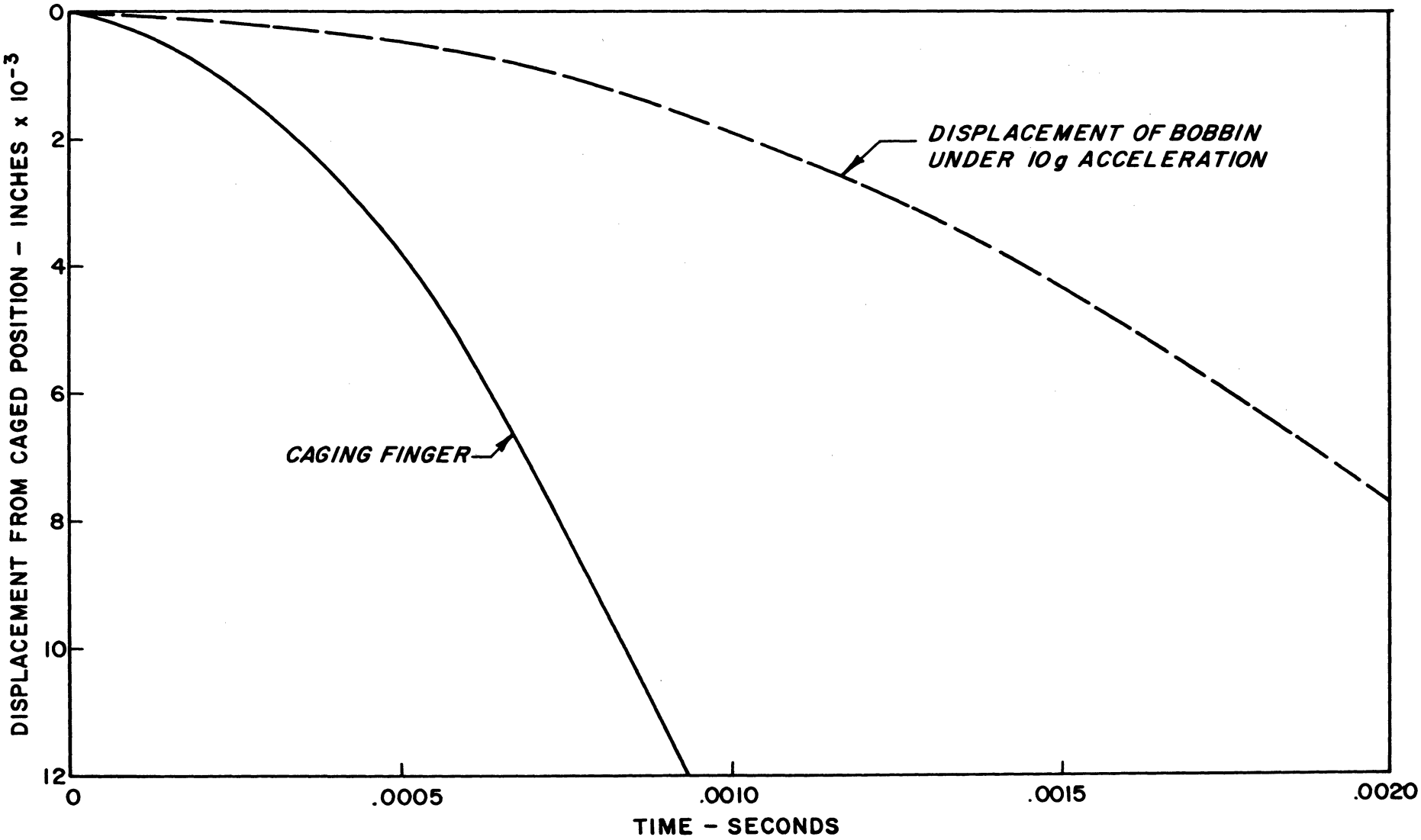

Fig. 9. Caging-finger displacement vs. time. Displacement spring 11, beryllium copper 0.020 in. thick, micro-switch mode.

acceleration is greater than that of the bobbin. However, to promote constant lag time and low initial velocity the time of break-free from the stops should be kept within measured acceptable limits. A setup to measure this parameter was made. The accelerometer was positioned so that the caging stroke was on a vertical axis. A variety of weights, simulating larger-than-one-g conditions, was screwed on the caging finger. The accelerometer was then cycled. The time from field collapse to break-free from the stops was measured. The results were as follows:

TABLE I

BREAK-FREE TIME IN MILLISECONDS

Voltage	Axis	Added Weight in Grams			
		0	62.2	169.8	294.3
6	Horiz.	.8			
6	Vert.	.8	.8	.8	.8
7.5	Horiz.	.75-.8			
7.5	Vert.	.8 - .9	.8	.75-.8	.8 - .9

No weights were added in the horizontal position because of the unduly large frictional force imposed by the cantilevered load. This test also demonstrated the ability of the accelerometer to pick up the weights with applied voltages somewhat less than the planned figure of 8 volts.

2.4 REBOUND

As anticipated, the caging fingers were found to rebound into the cavity volume after the termination of the retraction stroke. A lead seat behind the caging head had been provided to damp the rebound but proved to be inadequate. Room for an additional damping pad existed at the other end of the fingers, and various devices and materials were tried in this space: springs and pads of Bakelite, Lucite, sponge rubber, Teflon, and polyureathane. The latter material proved to be satisfactory under long periods of operation. It has the one disadvantage of remaining compressed after long storage in the compressed state but this is easily handled by installing new pads on occasion. Figures 10 and 11 show the undamped and damped rebound of the fingers compared with the bobbin displacement, both as a function of time.

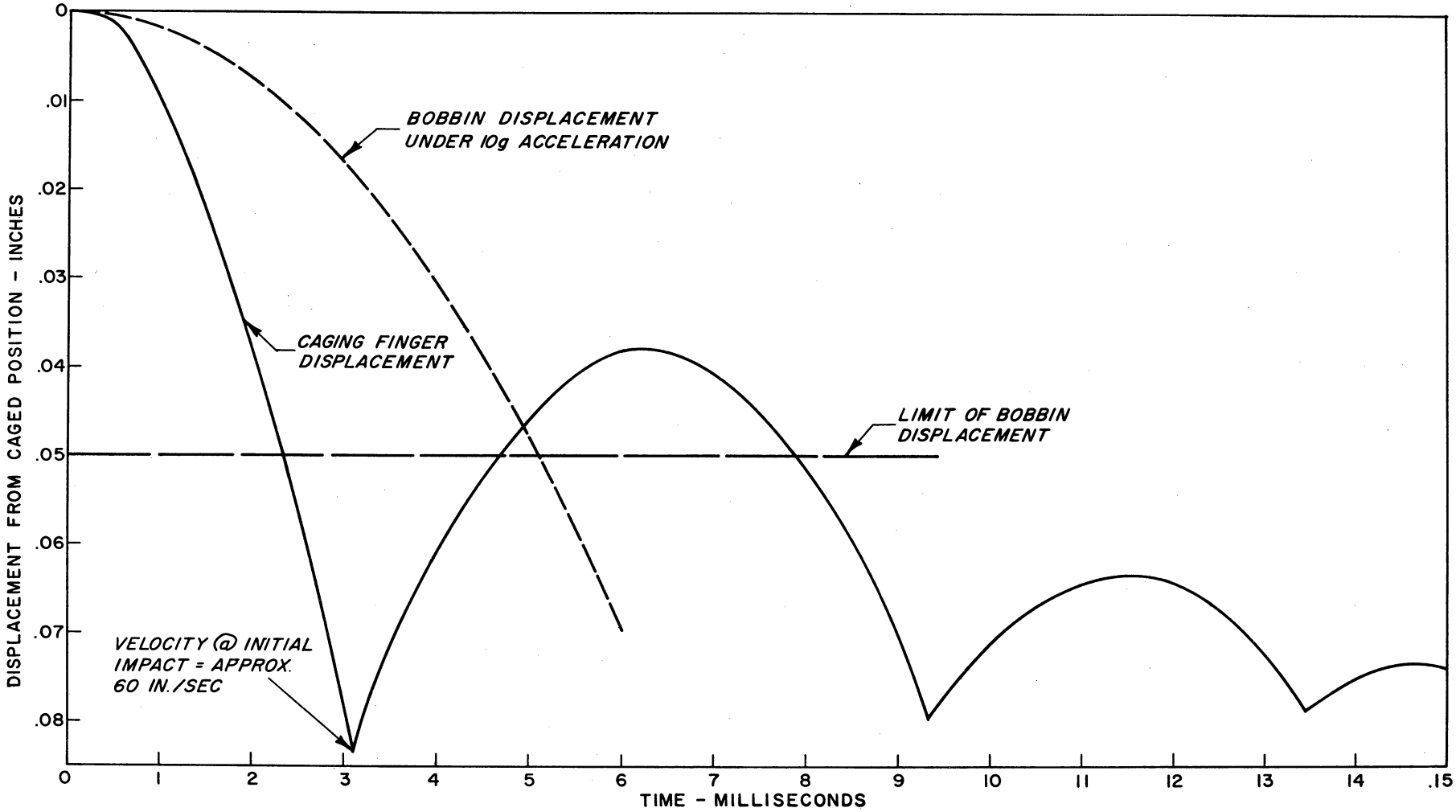

Fig. 10. Caging-finger displacement vs. time, showing rebound. Displacement spring 11.

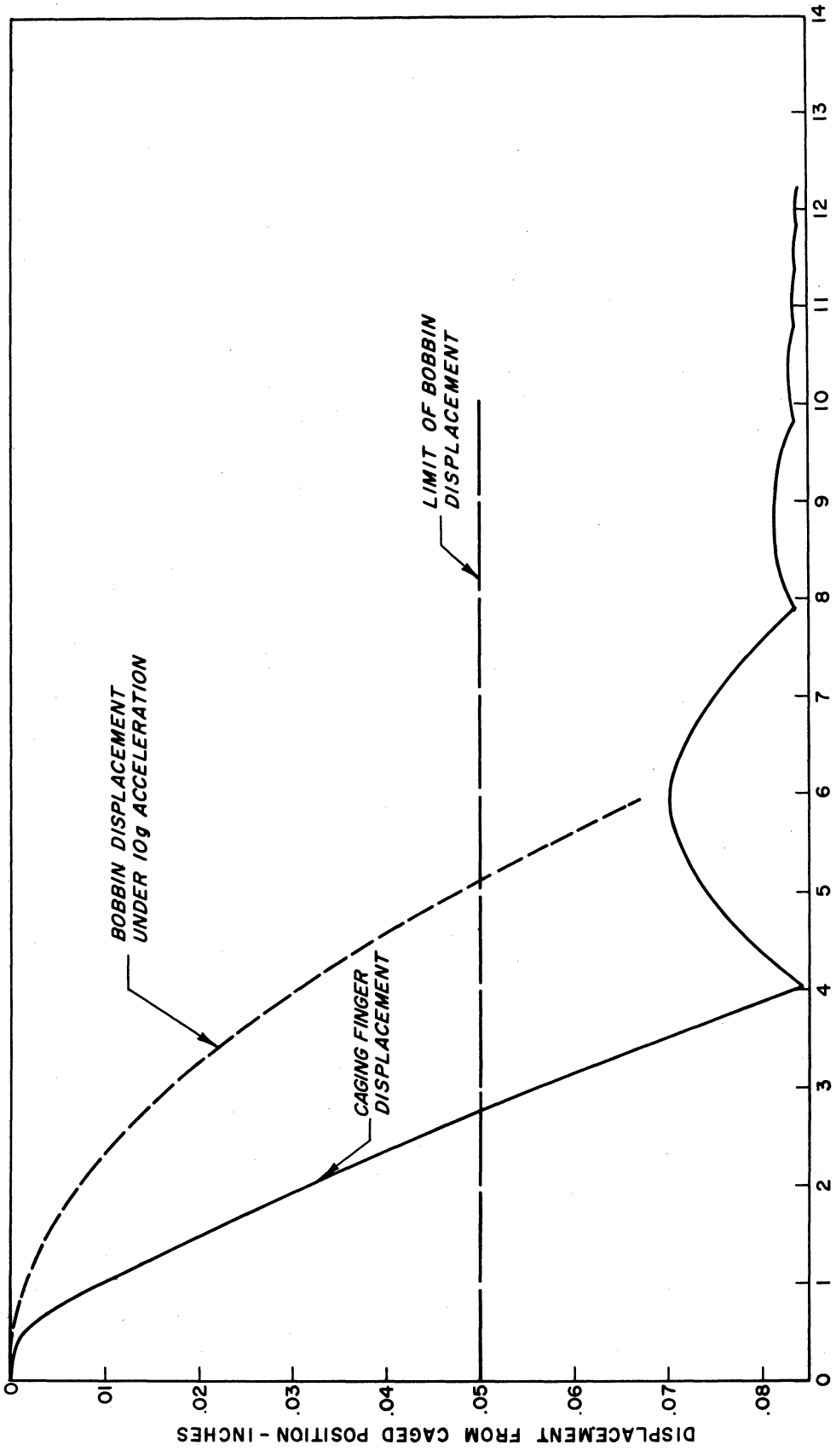

Fig. 11. Caging-finger displacement vs. time, showing rebound. Displacement spring 11.

3. ACCELEROMETER PRE-FLIGHT TESTING

3.1 TESTS AT 1 g

The majority of tests of the accelerometers was made on the bench at 1 g. In addition to representing an important region of the accelerations encountered in flight and of course being the easiest to perform, tests at 1 g are most important in discovering errors in centering, under and over-caging, errors in dimensions, and operational malfunctions. Past experience, reaffirmed by the work on these accelerometers, has indicated that an accelerometer performing properly at 1 g will do so at lower and higher accelerations as well.

The transit times may be measured from the oscilloscope (Tektronic 545) trace obtained with the moving vane described above, or more conveniently, with an electronic counter (Hewlett-Packard 522B). In the latter case the oscillator-detector circuit used in the low g drop test described below is used to trigger the counter on the sharp rise time of actual contact. The necessary gain was achieved with the transistor amplifier of Fig. 12. The circuit will trigger on a pulse of 0.2 volt with a fall time of 20 μsecs/volt. The performance of two of the accelerometers which is typical of all four is given in Tables II and III for various orientations. The standard deviations in 10 trials are shown. The average transit times in the various positions may be compared with the predicted transit time of 16.09 milliseconds.

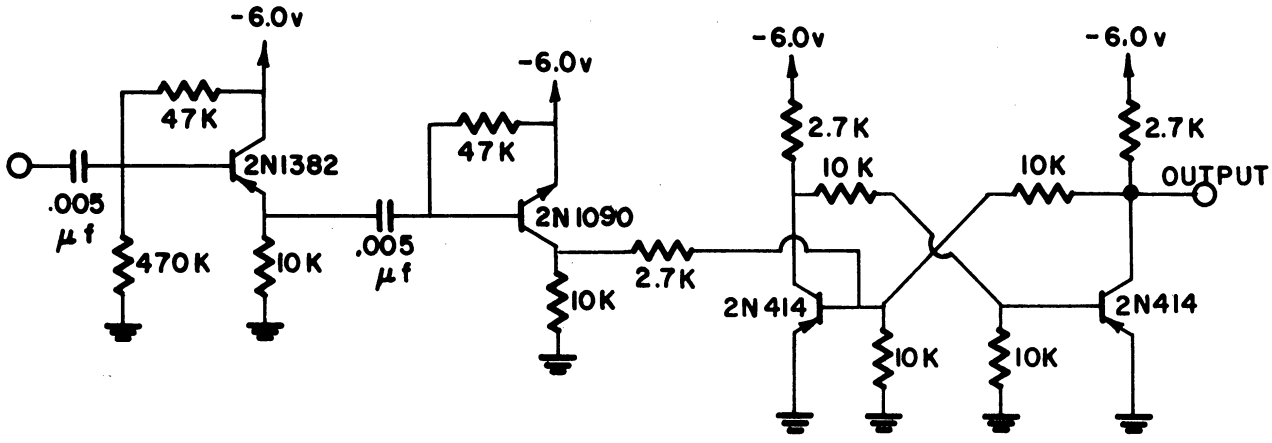

Fig. 12. Transistor pulse amplifier used in drop test.

TABLE II

ACCELEROMETER NO. 103

Transit Times at 1-g Acceleration

Transit Distance: .050 in.

Calculated Time: 16.09 millisec
Lag Time: 0.80 millisec
16.89 millisec

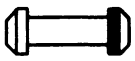

16.99	.09	.0049
16.91	.01	.0001
16.93	.02	.0004
16.89	.03	.0009
16.91	.01	.0001
16.85	.07	.0049
16.89	.03	.0009
16.90	.02	.0004
16.95	.03	.0009
16.99	.07	.0049
169.22		.0184

$\sqrt{.0018} = .043$

.043 ÷ 16.92 = .25%

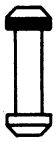

16.89	.00	.0000
16.95	.06	.0036
16.86	.03	.0009
16.90	.01	.0001
16.87	.02	.0004
16.92	.03	.0009
16.84	.05	.0025
16.93	.04	.0016
16.89	.00	.0000
16.90	.01	.0001
168.95		.0101

$\sqrt{.001} = .033$

.033 ÷ 16.89 = .19%

16.76	.05	.0025
16.73	.08	.0064
16.70	.11	.0121
16.80	.01	.0001
16.95	.14	.0196
16.79	.02	.0004
16.87	.06	.0036
16.88	.07	.0049
16.79	.02	.0004
16.85	.04	.0016
168.09		.0516

$\sqrt{.0052} = .072$

.072 ÷ 16.81 = .42%

16.77	.01	.0001
16.83	.07	.0049
16.71	.05	.0025
16.76	.00	.0000
16.72	.04	.0016
16.82	.06	.0036
16.81	.05	.0025
16.75	.01	.0001
16.70	.06	.0036
16.73	.03	.0009
167.59		.0198

$\sqrt{.002} = .045$

.045 ÷ 16.76 = .29%

16.69	.12	.0144
16.77	.04	.0016
16.76	.05	.0025
16.77	.04	.0016
16.86	.04	.0016
16.71	.10	.0100
16.91	.10	.0100
16.82	.01	.0001
16.88	.07	.0049
16.89	.08	.0064
168.06		.0531

$\sqrt{.0053} = .073$

.073 ÷ 16.81 = .43%

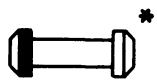

16.78	.08	.0064
16.84	.02	.0004
16.85	.01	.0001
16.81	.05	.0025
16.88	.02	.0004
16.89	.03	.0009
16.85	.01	.0001
16.91	.05	.0025
16.89	.03	.0009
16.87	.01	.0001
168.57		.0143

$\sqrt{.00143} = .038$

.038 ÷ 16.86 = .23%

*90°

TABLE III

ACCELEROMETER NO. 104

Transit Times at 1-g Acceleration

Transit Distance: .050 in.

Calculated Time: 16.09 millisec
Lag Time: 0.90 millisec
16.99 millisec

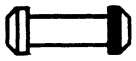

16.93	.11	.0121
17.11	.07	.0049
17.02	.02	.0004
17.09	.05	.0025
17.07	.03	.0009
17.20	.16	.0256
17.02	.02	.0004
16.97	.07	.0049
17.01	.03	.0009
16.97	.06	.0036
170.39		.0562

$\sqrt{.0056} = .07483$

.074 ÷ 17.04 = .43%

17.07	.02	.0004
17.01	.04	.0016
17.07	.02	.0004
17.01	.04	.0016
17.07	.02	.0004
17.04	.01	.0001
16.99	.06	.0036
17.08	.03	.0009
17.15	.10	.0100
17.05	.00	.0000
170.54		.0190

$\sqrt{.0019} = .04359$

.044 ÷ 17.05 = .26%

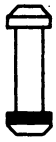

17.21	.00	.0000
17.24	.03	.0009
17.29	.08	.0064
17.22	.01	.0001
17.23	.02	.0004
17.17	.04	.0016
17.19	.02	.0004
17.19	.02	.0004
17.17	.04	.0016
17.21	.00	.0000
172.12		.0118

$\sqrt{.0012} = .035$

.035 ÷ 17.21 = .20%

17.01	.01	.0001
16.93	.07	.0049
16.94	.06	.0036
16.99	.01	.0001
16.95	.05	.0025
17.04	.04	.0016
17.02	.02	.0004
17.02	.02	.0004
17.02	.02	.0004
17.05	.05	.0025
169.97		.0165

$\sqrt{.00165} = .041$

.041 ÷ 17.00 = .24%

16.94	.02	.0004
16.94	.02	.0004
16.97	.01	.0001
16.94	.02	.0004
16.93	.03	.0009
16.95	.01	.0001
16.95	.01	.0001
16.99	.03	.0009
16.97	.01	.0001
17.01	.05	.0025
169.59		.0059

$\sqrt{.00059} = .024$

.024 ÷ 16.96 = .14%

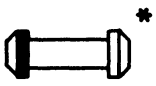

17.03	.03	.0009
16.98	.02	.0004
17.05	.05	.0025
17.01	.01	.0001
17.00	.00	.0000
17.03	.03	.0009
17.03	.03	.0009
16.98	.02	.0004
16.93	.07	.0049
16.96	.04	.0016
170.00		.0126

$\sqrt{.00126} = .036$

.036 ÷ 17.00 = .21%

*90°

3.2 LOW-ACCELERATION INVESTIGATIONS

Because the low-acceleration performance of the accelerometer determines the maximum altitude of density measurement of the sphere experiment, considerable effort in the program was expended on this factor. Initial velocity imparted to the bobbin by the release mechanism and initial velocity imparted to the bobbin as a result of its center not coinciding with the center of spin of the sphere are the two important sources of difficulty at low accelerations. The latter problem is approached by precision construction and careful balancing of the sphere, a process discussed below. Initial velocity imparted by the caging mechanism is a function of the design and quality of construction. In a completed accelerometer the initial velocity is most satisfactorily tested for in an implicit way by an over-all performance test in nearly free fall, i.e., in an Attwood's machine. In the previous report a different approach to checking for initial velocity was described but was not applied to this design, one reason being the impracticality of removing the center section. Consideration was given also to the possibility of testing the accelerometers at zero g in aircraft flying special trajectories. The zero-g condition lasts long enough so that eventual contact of the bobbin may be used to calculate the initial velocity and hence the error to be expected from such an initial velocity when using the accelerometer at a small acceleration which is not zero. The zero-g aircraft tests were beyond the scope of this contract and were not attempted.

The most promising approach appeared to be to construct a new Attwood's machine with extended range. The range was extended toward the low-acceleration end by using a new pulley of lower moment of inertia and a more massive bullet than in the previous machine. The moment of inertia of the new pulley was measured by the method of Ref. 3, that is, by measuring the time of fall of a small mass through a measured distance, the mass being attached to the pulley by a thread wrapped around the rim. The moment of inertia is given by

$$I = \frac{M_1 r^2 T^2 \left(g - \frac{2S}{T^2}\right)}{2S}$$

where

M_1 = mass of small mass

r = radius of pulley

T = time of fall

S = drop distance

I for the new pulley was found to be 662.64 gm cm^2 compared with 1002.02 gm cm^2 for the old. Now, using the new large bullet weighing 24,381 grams (vs. 7,171 for the old), a transit time for the accelerometer was found to be 446.6 milliseconds from

$$t = \sqrt{\frac{2s(M r^2 + I)}{gI}}$$

where

s = transit distance of accelerometer

M = mass of large bullet

This corresponds to an acceleration of $a = 2s/t^2 = 1.283$ cm/sec^2 or 0.00138 g.

To avoid errors in the acceleration due to heavy leads to the accelerometer coils, these were eliminated by incorporating the batteries in the bullet. The solenoids were controlled by means of a photocell circuit operated by light passing through a small opening in the bullet casing. The circuit is shown in Fig. 13. The photo-cell A is a self-generating type. When it is energized, the 2N456A conducts and energizes the solenoid coils. Shortly after the bullet is released by a trigger, it passes out of the beam of light, thus de-energizing the coils and releasing the bobbin. The bobbin transit time signals are carried in three small (0.004-in.-diam) wires leading from the bullet.

The bullet is 33 in. long and made of standard 4-in. pipe and couplings. The center section, made of brass, houses the accelerometer and auxiliary circuits. The accelerometer cavity is located on the c.g. of the entire unit to minimize centrifugal acceleration due to rotation of the bullet in fall. A special fork drop latch was devised to keep horizontal motion to a minimum. See Fig. 14. The bullet, accelerometer, and control circuit are shown in Fig. 15. Figure 16 shows the accelerometer mounted in the control circuit rack. A catch basket was built to prevent damage to the accelerometer and circuits in the bullet. It was designed to keep impact accelerations below 80 g. The construction is a tripod arrangement consisting of a shaped and padded ring free to slide vertically on three posts. The base of the ring is supported by three auto springs with shock absorbers inside. A large inverted pyramidal chute guides the bullet into the ring and prevents "fall over" damage. The catch pad is seen in Fig. 17.

Impact accelerations were measured with a Massa Laboratories crystal accelerometer Model M191 having the following characteristics: sensitivity 42

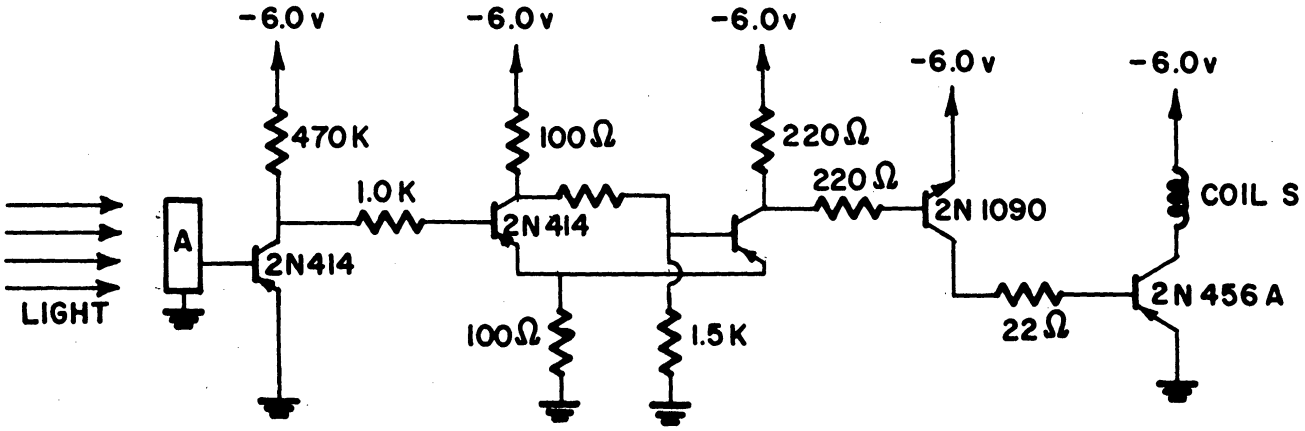

Fig. 13. Photocell and amplifier used to control accelerometer in drop tests.

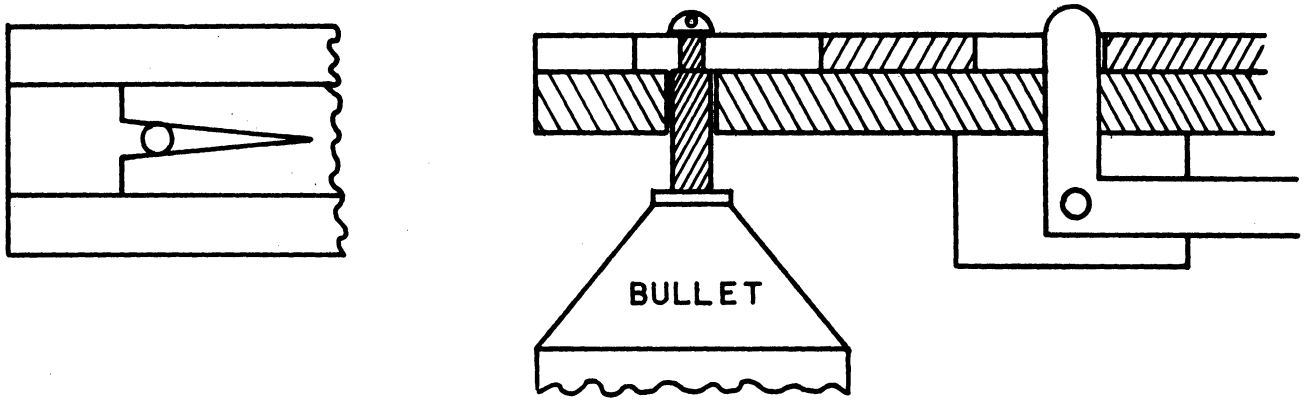

Fig. 14. Bullet release device for drop tests.

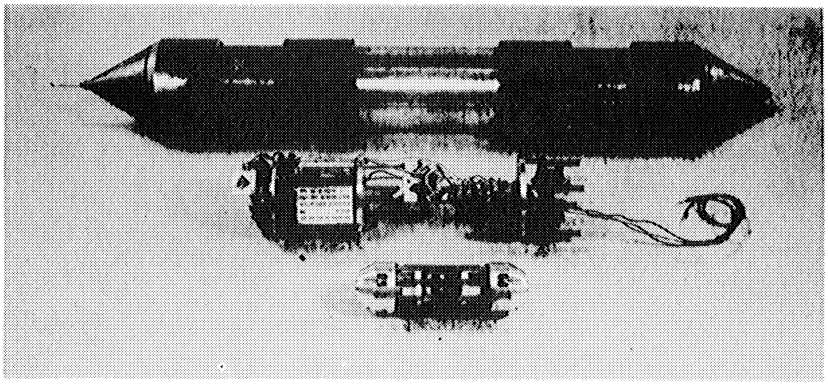

Fig. 15. Drop bullet, control circuit, accelerometer.

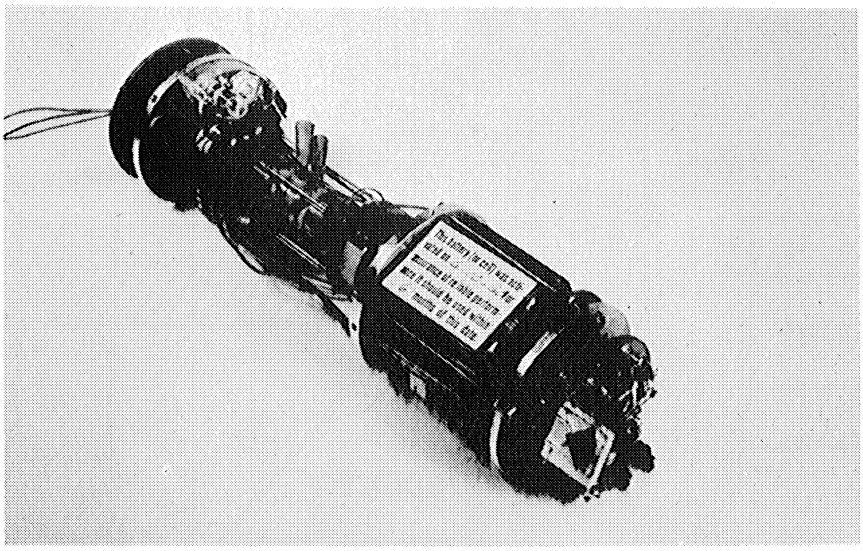

Fig. 16. Accelerometer mounted in control circuit rack.

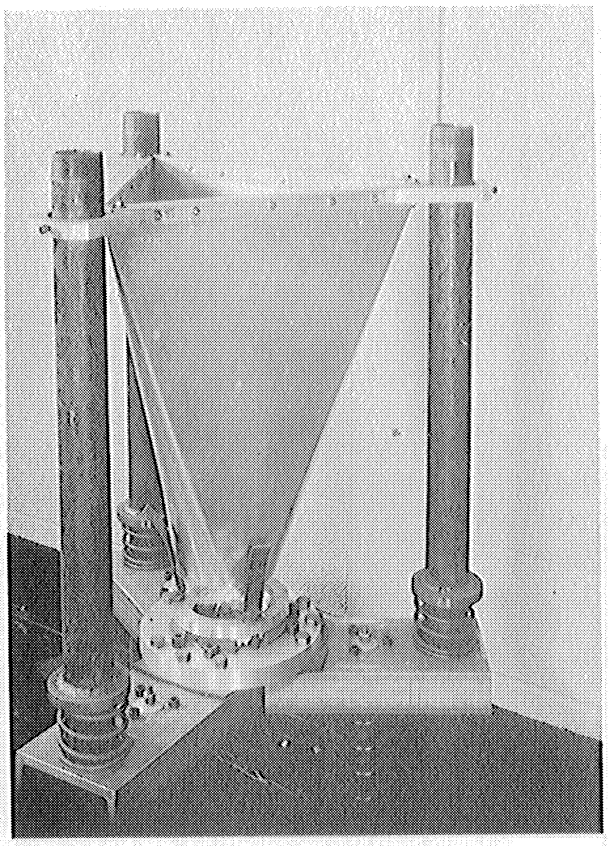

Fig. 17. Catch basket.

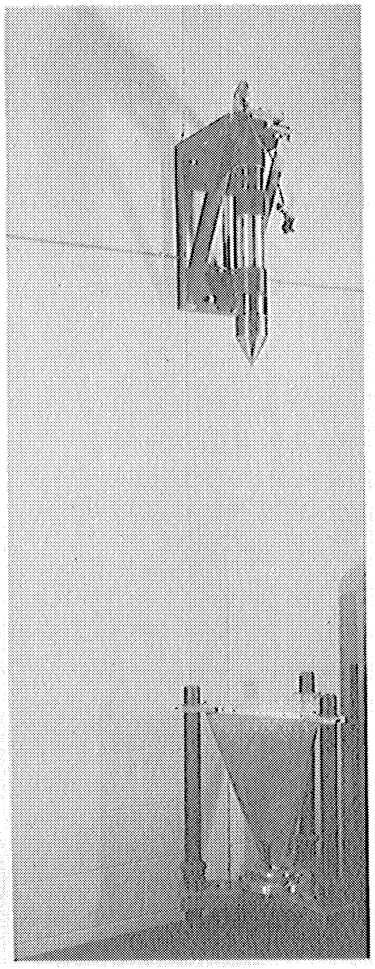

Fig. 18. Drop test setup.

millivolts/g; dynamic range 0.001 to 1000 g; resonant frequency 36 kc; frequency range 10 to 30,000 cps. First drops indicated accelerations of 122 g's, but this was reduced to 45 g's by the addition of padding in the catch device. The bobbin transit time of 446.6 milliseconds required a drop distance of 4 feet which, together with the dimensions of the apparatus, resulted in mounting the release mechanism about 10 feet above the floor. A heavy steel shelf holding the drop mechanism was attached to a vertical steel beam imbedded in the wall of the building. The over-all drop test setup is illustrated in Fig. 18. In making successful drops, attention to all the details noted in describing the use of the previous Attwood's machine was of even greater importance. It is reasonable to state that the adjustments and sources of error in the Attwood's machine were more troublesome than in the accelerometer. Since good agreement with the predicted transit times was finally achieved, the technique must be considered successful, although it is not a "calibration" in the sense that the errors may be ascribed to the accelerometer and corrected for. The technique is really a check of proper operation, after which the accelerometer is taken to be an absolute device whose performance is predicted from calculations based on dimensions. A typical population of five measures of a predicted transit time of 446.6 milliseconds (reading all digits presented by the counter) is:

	444.27
	448.87
	450.11
	447.92
	455.53
Avg.	449.3

4. SPHERE MECHANICAL DESIGN

4.1 ACCELEROMETER MOUNTING

Special consideration was given to mounting the accelerometer in the sphere because of the effect of the mount on bobbin centering and because the accelerometer acts as a diametral bolt which holds the sphere end bells tight to the center section against pressurization. The exterior length of the accelerometer is about 0.020 in. shorter than the interior sphere diameter (cap to cap). This dimension varies from sphere to sphere because of the accumulated effects of tolerances and strains. Centering of the accelerometer was accomplished as follows. The accelerometer was fully seated in one sphere cap with the cap screw tightened a specified amount as measured by a torque wrench. The second cap was then tightened with equal torque. The first cap screw is then loosened and the second one tightened with the same torque, the number of turns of the second screw required to do this being carefully noted.

The second cap screw is then backed off by one-half the measured turns. Finally the first cap screw is tightened with the same torque used throughout.

With one atmosphere pressure inside the sphere and vacuum outside the total force carried by the accelerometer as a tension member is about 500 lb. The accelerometer was designed in the first place to accommodate the load and did so reasonably well. However, small changes in transit time were sometimes noted between the pressurized and unpressurized conditions. The trouble was eliminated by separating the end caps of the accelerometer from the working parts and connecting the former with four 10-32 bolts. These carried the tension load leaving the accelerometer working parts unstressed.

4.2 BALANCE

The necessity for sphere balance has been discussed previously. In checking sphere balance it is assumed that the center of the bobbin is on the geometrical center of the sphere. Considering the tolerances used in machining the various parts, this is probably true to plus or minus one or two thousandths of an inch. The balancing operation then becomes one of getting the center of gravity of the sphere as close to the geometrical center as possible. In Table I of Ref. 7 the balance of previous spheres is shown. Distinction is made between the displacement of the c.g. from the center and from the spin axis because, if the sphere preserved its angular momentum about the spin axis (i.e., the longitudinal axes of the rocket and accelerometer), it would be more important to keep the latter displacement small. The range of these displacements in 14 spheres were, respectively, 0.003 in. to 0.050 in. and 0.001 in. to 0.025 in.; the later spheres were the better ones.

In the spheres of this report several techniques and changes were resorted to for improved balance. First, the intervalometer motor which may have had a gyroscopic effect was replaced with an electronic circuit. The only significant moving parts in the new spheres were the pick-up fingers. These are inherently symmetrical. However, the balance with the fingers advanced and retracted was checked and found unchanged. Another variable, the possible sloshing of electrolyte in the batteries was eliminated by having no excess electrolyte. Balance was measured with a Taylor Universal Static Balancing Machine seen in Fig. 19. It may be noted here that static balance of the sphere is all that applies because a freely falling body can rotate only about its c.g., i.e., it has no constraining bearings. Rough balance of the sphere was obtained by properly located lead weights in the form of plates and washers placed in both the body and caps of the sphere. Three trimming weights, adjustable from the outside with the sphere "buttoned up" were incorporated in one of the end bells of the spheres. These were used for final balance just before flight. The Taylor machine is calibrated to read unbalance in ounce inches. This reading, divided by the weight of the sphere in ounces (about 175) gives the c.g. displacement in thousandths of an inch. Corrections for the different masses of

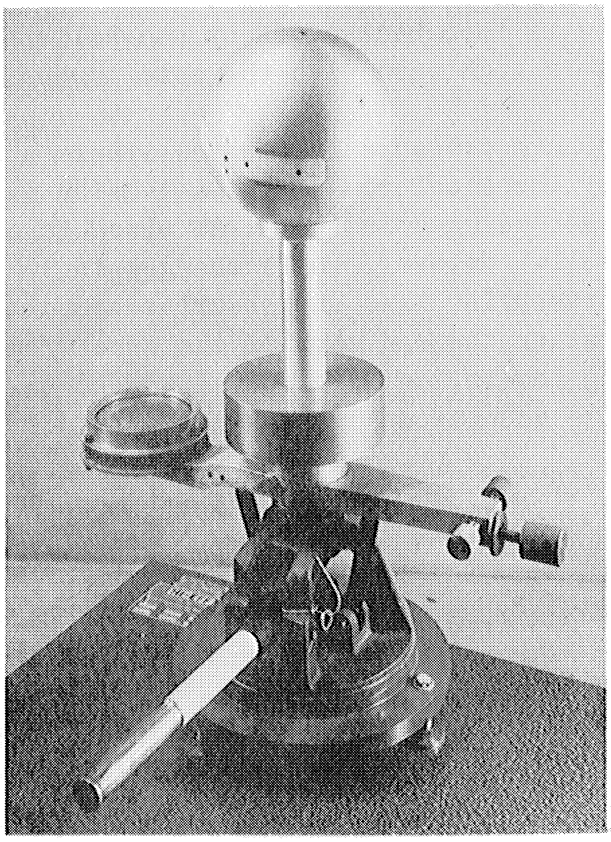

Fig. 19. Sphere on balance testing machine.

the individual spheres and for the mass of the adapting fixture must be made. Errors due to out-of-roundness of the spheres and air drafts in the room were noted at the point of best balance. Everything considered the c.g. in all the spheres was found to be within about ± 0.002 in. of the geometrical center. This compares with about the same figure for the tolerance of construction of the sphere and also is about as close as the balance machine could be practicably read. It should be noted that with different fixtures, the sensitivity of the balance machine can be improved. In checking balance the sphere was merely rested in the cuplike adapter fixture of the balance machine so that balance about any axes (two at a time) could be read on the spirit level with great ease. The balance machine saved many hours of labor over the previous system of suspending the sphere on a wire and observing it with a theodolite.

4.3 FLIGHT CONFIGURATION

The four spheres in their final flight configuration were nearly the same in mechanical construction as the earlier ones. The outside diameter remained at 7 inches. The antenna slot and components were unchanged. Internally, the end bells had minor changes to accommodate the new accelerometer end caps. One end bell was fitted with the externally adjustable balancing weights. The center section had some webbing removed. Four function outlets were used as before but only the rotary switch was unchanged. The ball starting switch was redesigned, the pressure port modified and the monitor plug was wired for battery charging.

Figure 20 shows the accelerometer in the center section of the sphere (antenna facing camera). The adjustable balance weights are in the right-hand bell with rough balance lead washers mounted underneath. In Fig. 21 the four function ports are shown.

5. SPHERE ELECTRONICS

The complete falling-sphere system is shown in block-diagram form in Fig. 22. Figures 23 through 27 show various sphere-construction details. This system can conveniently be broken down into six sections as follows:

1. Accelerometer
2. Contact detector
3. Intervalometer
4. Modulator
5. Accelerometer drive
6. Transmitter

The accelerometer with its two electrically isolated cavity sections has been completely described previously in this report. Along with the new accelerometer, is a newly devised capacity-actuated contact detector which provides a highly precise measurement of the time of accelerometer bobbin contact with the cavity wall. This is accomplished without the need for any physical connection between the bobbin and the rest of the accelerometer. The intervalometer is the basic controller for the system. It initiates and controls the following series of events:

1. Generates a periodic series of signals (called "clock pulses") which set the maximum rate at which the accelerometer can be recycled. These clock impulses are transmitted as 5-microsecond pulses. They serve to assist ground-station personnel in tracking the sphere during its trajectory with the ground-station telemetry antennas. The clock pulses are also useful as timing markers and should be particularly helpful if noise pulses are present on the telemetry records.

2. Generates a signal in synchronism with the release of the bobbin by the accelerometer caging fingers. This signal is transmitted as a 10-microsecond "start" (i.e., "release") pulse.

3. Prevents the system from recycling the accelerometer until after a "stop" (i.e., "contact") pulse has been received. If 2.5 seconds after bobbin release a stop pulse has not appeared, a stop pulse is simulated within the intervalometer and the accelerometer is recycled. The stop pulse is transmitted as a 20-microsecond pulse which completes the series of pulses trans-

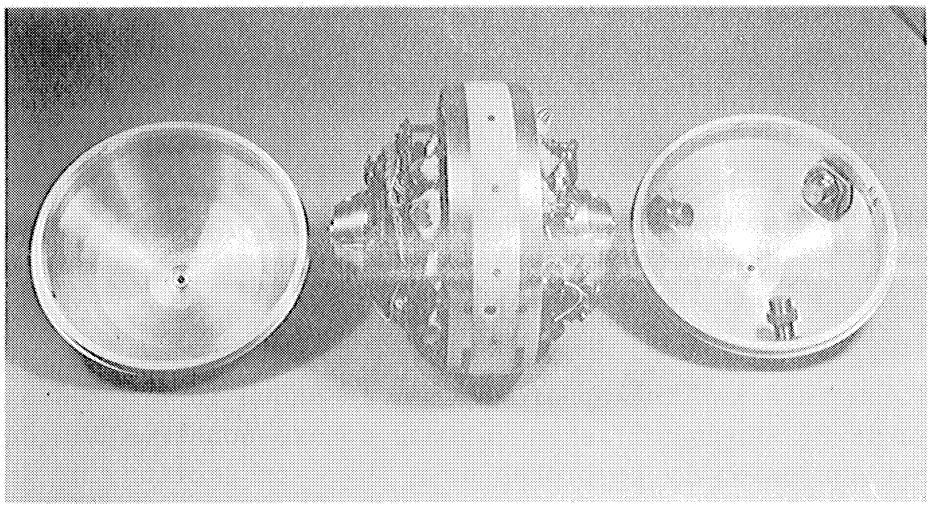

Fig. 20. Accelerometer mounted in sphere; adjustable balancing weights.

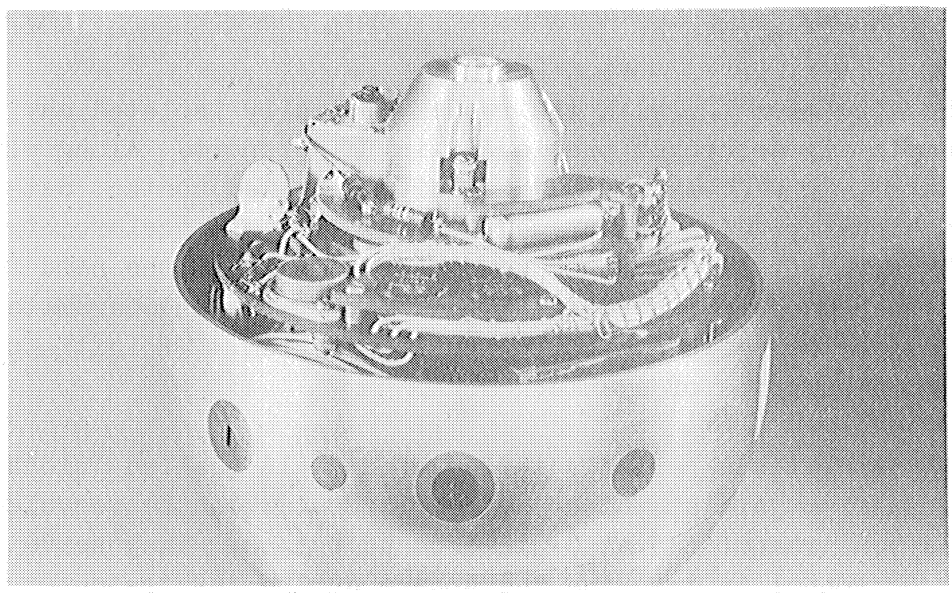

Fig. 21. Sphere, showing function ports.

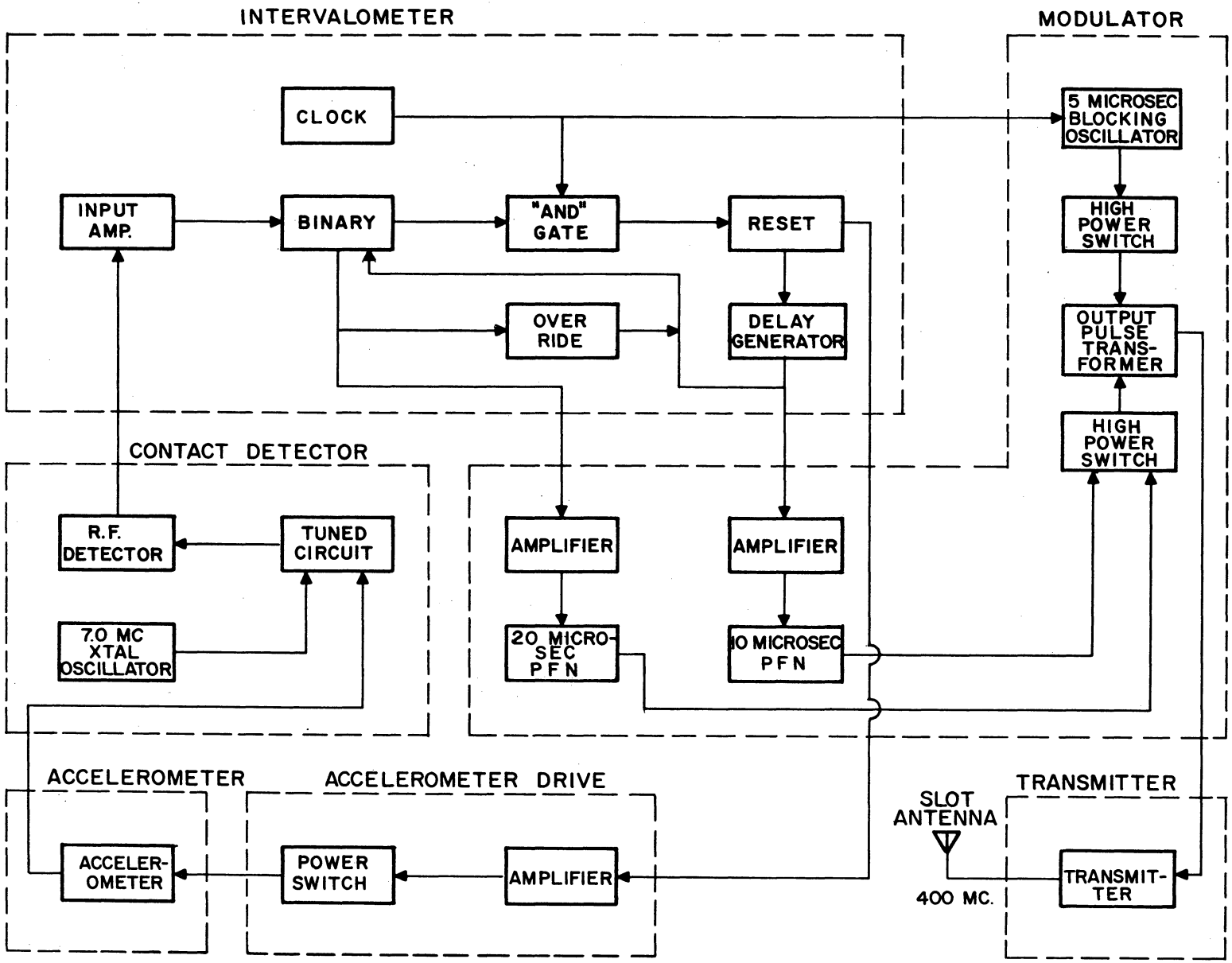

Fig. 22. Sphere circuit block diagram.

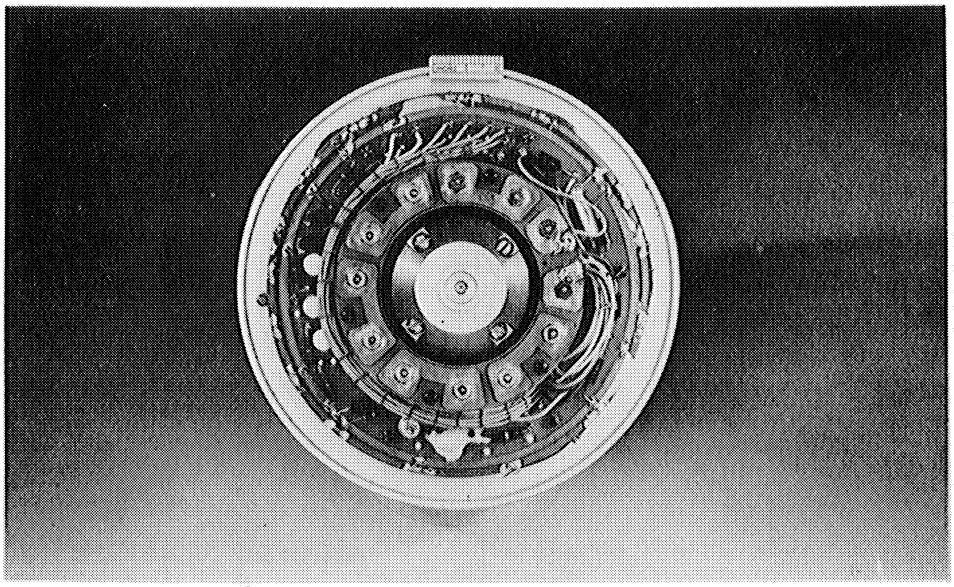

Fig. 23. Sphere with top bell removed.

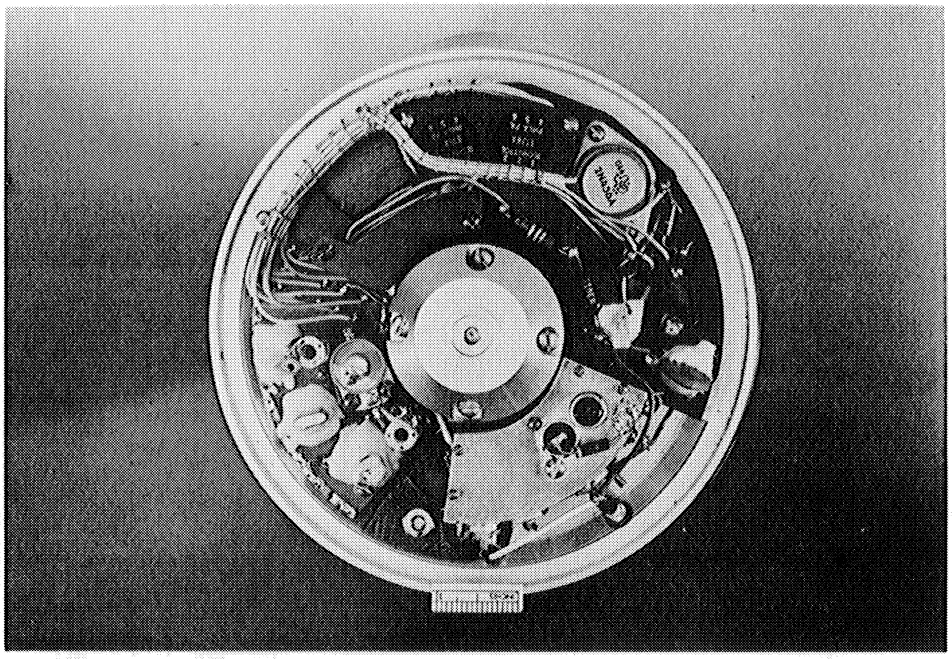

Fig. 24. Sphere with bottom bell removed.

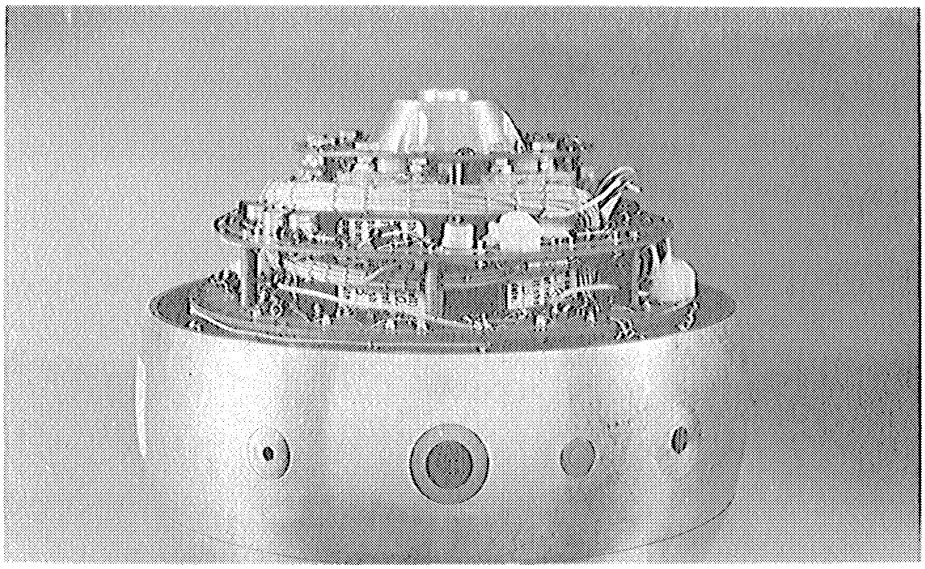

Fig. 25. Sphere with top bell removed, side view.

Fig. 26. Bottom view of sphere with accelerometer removed, output pulse transformer exposed.

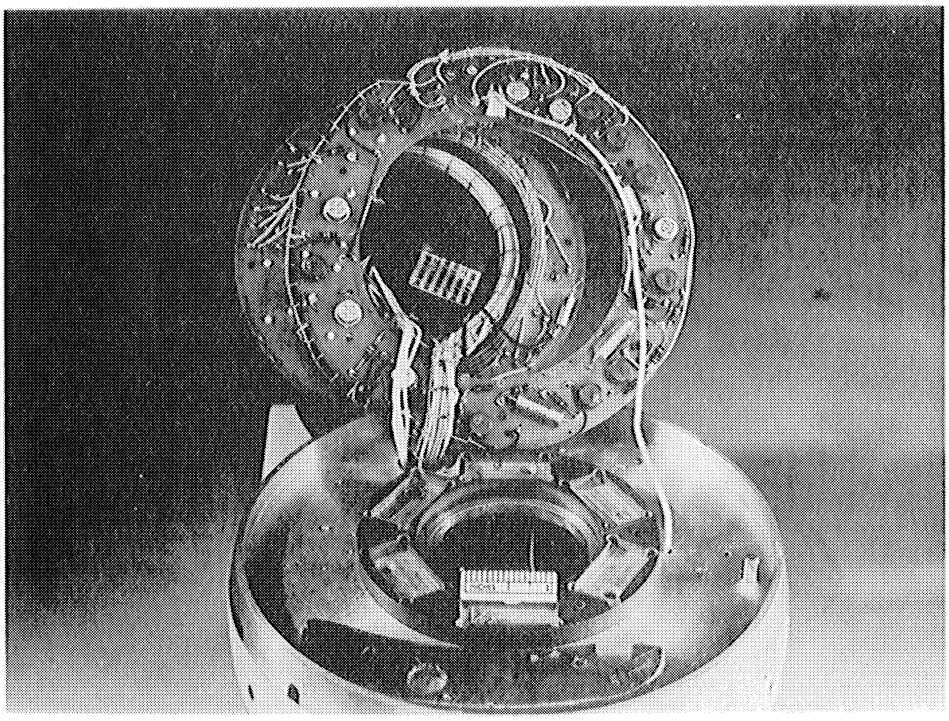

Fig. 27. Sphere with top electronics rings exposed.

mitted and received at the ground station.

In addition to the above, the intervalometer ignores minor detector output pulses which sometimes occur when the accelerometer caging fingers release the bobbin. It also neglects all outputs due to bobbin bouncing after initial contact has occurred. This system has been described as discretionary because the accelerometer does not normally recycle until after a stop pulse is generated by the bobbin. The discretion is not unlimited, however. After a stop pulse has been generated, the "and" gate remains closed until the succeeding clock pulse appears. Thus, accelerometer recycling is synchronized with the basic clock rate or integral intervals thereof. The above also applies whenever a mandatory accelerometer recycle occurs after a stop pulse does not appear within 2.5 seconds from bobbin release.

It will be noted from this description that in contrast to earlier falling spheres, a clock pulse has been added and both start and stop pulses are also "width-coded." Provision has also been made for longer bobbin transit times and faster accelerometer recycling than was feasible in the past. These features all assist in obtaining additional upper-atmosphere-density data over a wider range of altitudes, and facilitate data handling when either manual or automatic data reduction is undertaken.

All sections of Fig. 22 except the transmitter are described in detail below. The transmitter, operating at 400 megacycles with a peak pulse power output of approximately 15 watts, is identical with those used in earlier falling spheres. The reader is referred to Ref. 6 for additional details.

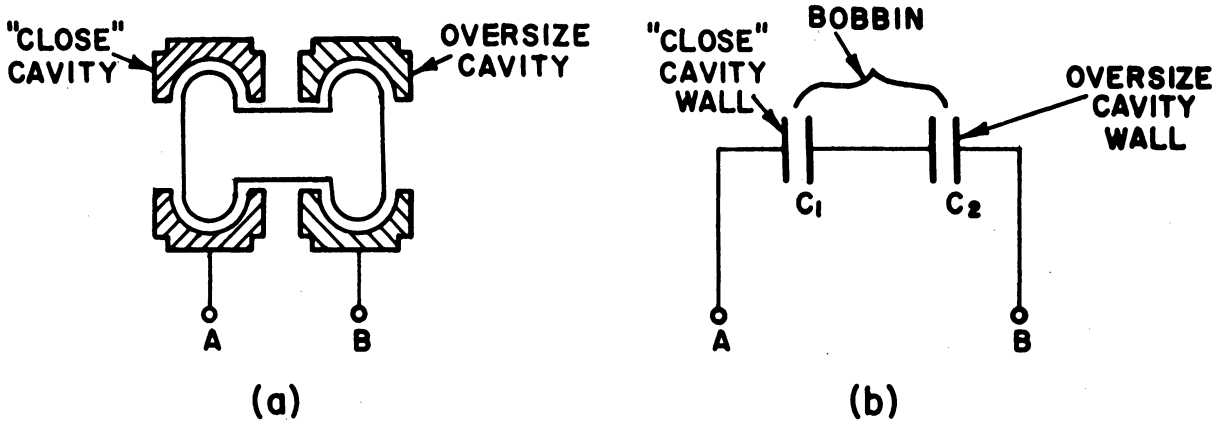

Fig. 28. Accelerometer bobbin-cavity capacitances.

5.1 CONTACT DETECTOR

The contact detector utilizes the change in capacitance between the electrically conductive bobbin and its two surrounding and electrically isolated cavities. Figures 28a and 28b illustrate the bobbin-cavity relationship and the equivalent electrical circuit. For simplicity, all fixed and stray C that does not vary with bobbin position within the cavities is not shown.

Consider now the variation of capacitance between terminals A and B of Fig. 28 as the bobbin moves in a direction which tends to increase C_1 while C_2 remains approximately constant. The capacity between A and B is given by:

$$\frac{1}{C_{AB}} = \frac{1}{C_1} + \frac{1}{C_2}$$

As the bobbin approaches the "close" cavity, C_1 increases, asymptotically approaching infinity in the limit. This means that at the instant of contact:

$$C_{AB} = C_2$$

A similar result occurs even when the cavities are the same size and C_2 is allowed to vary (as it generally does) in response to bobbin movement. Since C_1 varies approximately linearly with respect to the reciprocal of the distance between the bobbin and the cavity wall, it seems that C_{AB} would never be subject to discrete changes in value, even at bobbin contact. Consequently, if the capacitance variation is transformed into a varying voltage by appropriate associated circuitry, the rate of change of voltage with respect to bobbin position would be a function of bobbin velocity, and thus acceleration as well.

In fact, there should not be a pulse output at all, particularly at low acceleration levels. Fortunately, however, the above speculation has proved to be incorrect in actual practice. Extensive testing of the accelerometer and its contact detector at 1 g and at very low acceleration levels indicates that a contact pulse is always generated and its amplitude is independent of bobbin velocity.

The contact-detector circuitry shown in Fig. 29 consists of a 7.0-megacycle crystal-controlled transistor oscillator loosely coupled to a parallel-resonant tuned circuit. A peak responding diode detector and the accelerometer cavities are also connected across the parallel resonant circuit. C_{24} is adjusted so that when the bobbin is in its centered position and uncaged, the circuit is tuned somewhat off resonance. Any change in capacitance caused by bobbin movement will now affect the tuning of the resonant circuit and thus cause a change in the d-c output voltage of the peak responding diode detector.

The proposed mechanism responsible for the sharp discontinuity always observed upon bobbin to cavity contact is dielectric breakdown of the air when the distance between the bobbin and cavity becomes sufficiently small. In this event, the discontinuity at "contact" really occurs slightly before actual physical contact. However, the error thus involved amounts to less than 0.1% of the total transit distance. Extensive testing to confirm the above hypothesis has not been undertaken, but some experimentation and calculations have definitely indicated the possibility of a breakdown phenomenon.

The presence of C_{25} provides for more uniform contact pulses as a function of accelerometer orientation. When correctly adjusted, the maximum detector output is approximately 7 volts, which results in contact-pulse amplitudes of approximately 3 volts.

5.2 INTERVALOMETER

The operation of the intervalometer can be followed by referring to the circuit diagram, Fig. 29. To begin, assume that the circuit has been turned on, several recyclings have occurred, and that the bobbin is in transit. During transit, the binary is so set that the "AND" gate is turned off—i.e., no pulses can pass through the "AND" gate to trigger the RESET circuit. The clock circuit generates a pulse every 350 milliseconds which triggers the "clock pulse" modulator. The modulator generates a 5-μsec pulse and thus a "clock" pulse is transmitted.

When the bobbin makes contact with the cavity wall, a contact pulse is generated. This pulse, in the form of a "step" in d-c voltage, is transformed into an "impulse" (no d-c level) by differentiation and amplification in the input circuit. This impulse triggers the controlling binary (a bistable multivibrator) into its opposite state.

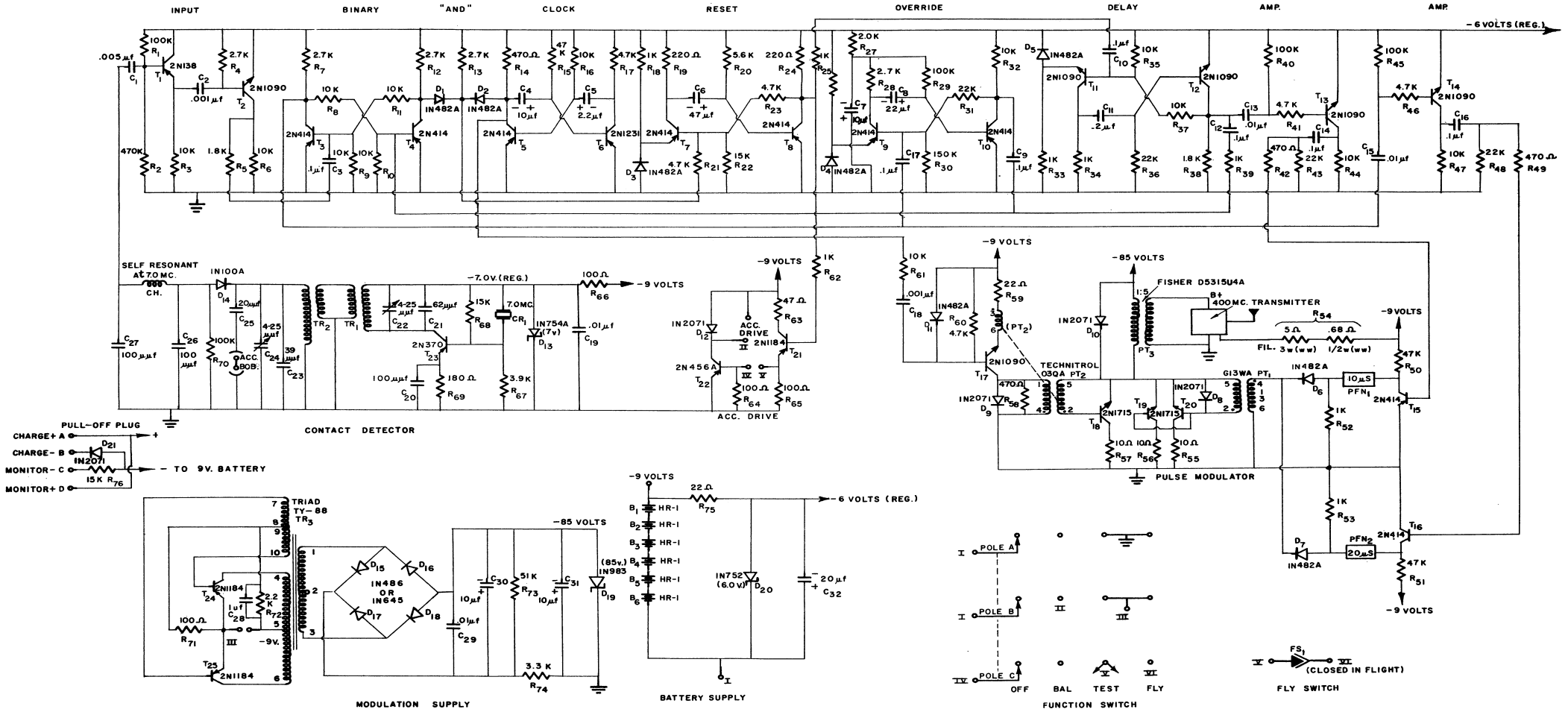

Fig. 29. Sphere-circuit schematic.

This change results in:

1. a 20-μsec pulse transmitted as a "stop" (i.e.,contact) pulse;
2. opening of the "AND" gate so that subsequent pulses can pass through;
3. resetting the circuit that provides for the simulated contact pulse.

As a result of (2), the next clock pulse will be allowed to pass through the "AND" gate and trigger the RESET circuit. The RESET is a mono-stable multivibrator, with a period of 150 milliseconds, with the primary purpose of energizing the accelerometer drive circuit for that period of time. At the end of this period the reset flips back to its stable state, the accelerometer drive circuit is de-energized, and the bobbin is released.

Upon returning to its normal state the RESET circuit triggers the DELAY circuit, another mono-stable multivibrator, into its quasi-stable state. The duration of the delay circuit period is about 2.5 milliseconds which delays resetting the controlling binary by this amount of time after the bobbin pick-up fingers have been de-energized. As the delay circuit returns to its normal state it resets the controlling binary to its original state so that it may be triggered by the next contact pulse.

The delay circuit is required because the fingers do not pull free of the bobbin the instant that the accelerometer coils are de-energized. In fact, it takes from 0.7 to 1.5 milliseconds for this to take place, depending on the finger spring adjustments. Occasionally on this break-away, minute bouncing between fingers and bobbin may occur. This bouncing is sufficient to cause small "contact pulses," which can appear to the intervalometer as true contact pulses if some way is not devised to ignore them. This is accomplished by the delay circuit which does not set the binary to accept a contact pulse until well after the fingers have pulled away from the bobbin.

Upon triggering of the delay circuit, the step voltage so generated is amplified and in turn triggers the 10-microsecond modulator, and a "start pulse" is transmitted. This occurs at the same instant that the accelerometer coils are de-energized. To correct for true release (when fingers withdraw from bobbin), the time it takes for the fingers to withdraw (the 0.7 to 1.5 milliseconds noted above) from the bobbin is measured accurately and is subtracted from all subsequent transit-time data points. This lag time apparently remains constant for a given adjustment of accelerometer springs.

As described so far, if a contact pulse failed to appear or was inadequate for initiating circuit action in the intervalometer, the accelerometer would never again be recycled. To insure against this disastrous possibility, a circuit is utilized that provides automatic recycling in the form of an over-ride circuit. This, again, is a monostable multivibrator, with a time period of 2.5 seconds. The over-ride is triggered into its quasi-stable state by the binary as the binary is being reset. When a contact pulse flips the binary, the over-

ride is returned to normal by the binary [(3) above]. However, if no contact pulse appears after 2.5 seconds have passed, the over-ride circuit automatically returns to its normal state, and upon so doing triggers the binary in exactly the same manner as would a contact pulse. From here the operation of the system is identical to that of a true contact-pulse-triggered binary action. With this over-ride circuit the system keeps on operating even if a contact pulse is missed. Thus once the system gets started it will keep recycling the accelerometer whether or not a contact pulse is received.

The intervalometer system always starts correctly because the normal action of monostable multivibrators is to be momentarily in their quasi-stable state when power is first turned on. They remain in this state for 1/4 to 1/2 of their normal period, then flip back into their normal state. Of course, when the delay circuit functions, it sets the binary in the proper state to accept a contact pulse; and this in turn sets the over-ride in its proper state to carry out its function. Meanwhile this turn-on action is taking place in the reset circuit which picks up the bobbin, centers it, and then releases it when the reset circuit returns to its normal state. From this point on circuit operation is as described above.

Referring to the detailed circuit diagram, the input circuit consists of an emitter follower buffer stage, T_1, followed by a differentiating-amplifying configuration. The primary purpose of C_1 is as a d-c block; however, along with the approximately 50K input impedance of the buffer stage, it helps to differentiate the contact pulse. C_2 along with R_4 and the input impedance of T_2 constitute the main differentiating circuit. T_2 amplifies the differentiated waveform and passes it on to the base of T_3. The action of T_2 is similar to that of a switch, in that it is normally cut off, but in heavy conduction during the contact pulse. The purpose of the input circuit is to take the d-c voltage containing the contact pulse, and change the contact pulse into a single "spike" waveform with which to trigger the binary. C_3 is present to block any d-c current which might tend to flow into the base of T_3, and R_5 is a current limiting resistor to protect the base of T_3 against high currents when T_2 and T_3 are both conducting.

The binary is a standard Eccles-Jordan type bistable multivibrator. Commutating capacitors were found unnecessary since switching speed without them was less than 2 microseconds, and speeds greater than this in this part of the system were not needed. Since most signals to and from the binary are of a pulse-type nature, capacitor coupling is used. The exception is the coupling to the "AND" gate, where standard low-level d-c logic has been employed.

Proper operation of the "AND" gate depends upon a greater voltage across D_1 in series with T_4 during conduction than appears across D_3 in series with T_7 during conduction.

The binary is triggered by a contact pulse when T_4 is conducting and T_3 is cutoff. The contact pulse appears as a negative spike at the collector of

T_2, and thus is transmitted to the base of T_3. This action turns T_3 on, thus cutting T_4 off. This in turn cuts D_1 off. However, if T_5 is still conducting, essentially all the 6 volts appear across R_{13}. But when T_5 becomes cut off, D_2 also is cut off and current then flows through R_{21}, thus turning T_7 on and triggering the reset circuit into its quasi-stable state.

Thus when either T_4 or T_5 is conducting, the reset circuit cannot be triggered into its quasi-stable state; but when both T_4 and T_5 are cut off, the reset is triggered and the accelerometer is thereby recycled.

T_5 is part of the clock circuit, which is an unsymmetrical astable multivibrator. The clock has a period of 350 milliseconds, T_5 being cut off during the 10-millisecond clock pulse.

Due to the extremely long time constant of C_4 and R_{15}, and the resulting low current in R_{15}, I_{CO} leakage current in T_6 resulted in very poor temperature stability of the clock circuit when germanium transistors were used.

We had to resort to silicon transistors, which eliminated much of the temperature instability. Still better stability was obtained by choosing capacitors for C_4 and C_5 (primarily C_4) with temperature coefficients which would best offset the transistor temperature dependence. The resulting circuit exhibited a total change of less than .5% period variation over a 40°F temperature range. Careful temperature compensation of T_5 was unnecessary due to the relatively short time constants involved with this transistor.

The reset circuit is a standard monostable multivibrator, with one slight modification. Normally a well-designed monostable multivibrator requires two separate power supplies: the normal collector supply voltage, and an opposite polarity supply for base bias through R_{22}. If transistor T_7, does not remain in the cut-off state, the circuit may become unstable and tend to oscillate. Because of weight and space-saving considerations, it was not practical to consider a separate power supply, and other methods of accomplishing the same end were investigated. The method finally settled upon was that of simulating an additional low-voltage power supply as illustrated by the R_{18}, D_3 combination. D_3 is a silicon diode, and in the configuration as used always has a forward conduction voltage drop across it of about 0.5 volt. With R_{22} returned to ground, T_7 will always remain in the cut-off state as long as T_8 is conducting and no trigger pulse is applied. This method exhibits no indication of instability and has been extremely reliable.

The reset circuit is a fairly low impedance (high-power) circuit. By making this a relatively high-powered logic circuit, only one intermediate stage of current amplification (T_{21}) is needed to drive switching transistor T_{22} used to supply the 3 amps necessary to recycle the accelerometer. The output point of the reset circuit is the T_8 collector, which drives the base of T_{21} in the accelerometer drive circuit and also triggers the base of T_{11} in the delay circuit.

The over-ride circuit is very similar to the reset circuit. A point of interest about the over-ride circuit is the decoupling network, consisting of R_{27} and C_7, associated with the collector of T_9 and the base of T_{10}. The over-ride circuit was purposely made a high-impedance circuit since the drive requirements on it were small. Consequently low-level pulses can trigger this circuit. In the course of operation of all the circuits in the system, rather high-level pulses drop the terminal voltage of the battery source enough to produce small pulses on the 6-volt regulated line. Occasionally these pulses become large enough to trigger the base of T_{10} through R_{28} and R_{29}. The decoupling network of R_{27} and C_7 eliminated this problem. No other circuit was faced with this problem as no other circuit attained nearly as high an impedance level as did T_{10} of the over-ride circuit. R_{26} and D_4 serve the same purpose in the over-ride circuit as R_{18} and D_3 do in the reset circuit. The binary is the drive and load circuit for the over-ride.

The delay circuit is also a standard monostable multivibrator, with D_5 and R_{33} serving the same purpose in this circuit as D_3 and R_{18} do in the reset circuit. The biggest difference between this circuit, the reset and the over-ride circuits is that NPN transistors are used here, whereas PNP transistors are used in the other two circuits. PNP transistors were arbitrarily selected for most of the circuitry. However, NPN transistors were employed wherever their use would simplify triggering, driving, or any other phase of the logic system. The delay circuit is such a case. The triggering pulses available, and the output pulses needed, suggested that NPN circuitry would be simpler and more efficient in this case.

The delay circuit is triggered into its quasi-stable state by the collector of T_8 of the reset circuit through R_{25} and C_{10} as the quasi-stable state time of the reset circuit terminates and T_8 switches from the "off" state to the "on" state. The step voltage generated as the delay circuit switches into its quasi-stable state triggers the 10 microsecond pulse modulator and a start pulse is transmitted. After 2.5 milliseconds the delay circuit switches back to its normal state, and upon so doing provides a negative pulse to the base of T_4 through R_{39} and C_{12}, turning T_4 back on (and T_3 off) so that the next contact pulse can again turn T_3 on. This latter action by the delay circuit also aids in turning T_{10} of the over-ride circuit off (thus initiating the quasi-stable state in the over-ride circuit), but the main drive for this action comes at the base of T_9 from the binary through C_{17} as the binary is being reset by the delay circuit.

5.3 MODULATOR

The section of the system block diagram entitled modulator processes the stop, start, and clock pulses so that they may be transmitted as 20- , 10- , and 5-μsec pulses, respectively. The stop-pulse step voltage is amplified and impressed upon a 20-μsec pulse forming network (PFN), and the start-pulse step

voltage is amplified and impressed upon a 10-μsec PFN. The clock pulses are used to trigger a 5-μsec blocking oscillator. The resulting 20- , 10- , and 5-μsec pulses are then used to drive high-power switches so that high-power 20- , 10- , and 5-μsec pulses are placed across the primary of a power pulse transformer. The secondary of this transformer provides the B+ voltage for the transmitter.

Referring to the circuit diagram, the start-pulse step voltage is amplified by T_{13} and its associated circuitry; the stop-pulse step voltage, by T_{14}. The principal components of the two pulse-forming networks are: (1) T_{15} and PFN_1 for the 10-μsec start pulse, and (2) T_{16} and PFN_2 for the 20-μsec stop pulse. Operation of the 10-μsec unit is as follows: Due to capacitor C_{14} and resistor R_{43}, T_{15} is normally cut-off. PFN_1, being a lumped-constant open-circuit 5-μsec delay line consisting of series-parallel combinations of inductance and capacitance, charges up to the full 9 volts supply voltage, so that no current flows in R_{52} and D_6. The charging path of PFN_1 is through R_{50} and R_{52}. The amplified start-pulse step voltage is applied to the base of T_{15}, thereby switching T_{15} into the saturated conduction state. PFN_1 then discharges through T_{15}, D_6, and the primary of PT_1 for 10-μsec. The reflected PT_1 load, along with the saturation resistance of T_{15} and R_{52}, constitutes the proper load for PFN_1. Thus no reflections occur and one-half of the original PFN_1 voltage (4.5 volts less the transistor drop of about 0.1 volt) appears across the primary of PT_1 for 10-μsec. Upon complete discharge of PFN_1 the voltage across PT_1 terminates abruptly, D_6 becomes nonconducting, and the saturating current for T_{15} is supplied by the supply voltage (-9 volts) through R_{50}. Finally, when the drive current on the base of T_{15} terminates, T_{15} again cuts off, and PFN_1 charges up to -9 volts again through R_{50} and R_{52}, and the circuit is ready for another start pulse. Recharging time of the PFN is about 10-μsec. Operation of the 20-μsec unit is identical except that it is triggered by the amplified stop pulse step voltage and has a 20-μsec output.

The diodes D_6 and D_7 prevent pulse feedback to the opposite PFN. The pulse transformer PT_1 transforms the 4.4-volt, 10-μsec (or 20-μsec pulse down to 1-1.5 volts. In this manner maximum current drive to the bases of T_{19} and T_{20} is achieved along with approximately properly matching the 100-ohm characteristic impedance of the delay lines. D_8 prevents excessive back voltage on the base to emitter junctions of T_{19} and T_{20} due to induced voltages in the secondary of PT_1. The 10- and 20-μsec signals applied to the bases of T_{19} and T_{20} are sufficient to drive these normally cut-off transistors into conduction saturation. This forces the complete 85 volts (less the voltages drops in R_{55} and R_{56} and the drops in T_{19} and T_{20}) across the primary of PT_3, the output power pulse transformer. This voltage is transformed by PT_3 into the 360 volts needed for the transmitter B+. D_{10} serves the same sort of function as D_8 in that it protects T_{19} and T_{20} against wrong polarity voltages from collector to emitter. The purpose of R_{55} and R_{56} is equalization of currents through T_{19} and T_{20}. Total current through the primary of PT_3 during conduction is 0.8 amp.

Saturation resistance of the 2N1715 is about 10 ohms. Absolute maximum rated current for 2N1715 is 1.0 amp. However, it was found that 2-2N1715 used in the parallel configuration as shown in the circuit diagram required less base drive current for the same saturation characteristics—thus the use of the parallel configuration. The use of 2 transistors in place of 1 also affords some degree of redundancy.

The 5-μsec pulse is generated when the leading edge of the 10-millisecond clock pulse triggers the base of T_{17} through R_{61} and C_{18}. The configuration of T_{17} is that of a blocking oscillator with the feedback winding in the emitter. The output of the blocking oscillator is applied between base and emitter of T_{18}, and is a 5-μsec pulse of enough power to switch T_{18} from cut-off into conduction saturation. This, of course, applies a 5-μsec B+ pulse on the transmitter in exactly the same manner that T_{19} and T_{20} do the 10- and 20-μsec pulses. Width control of the transmitted clock pulse is possible by adjusting the value of resistance R_{59}. As R_{59} is made smaller, the pulse width becomes larger and vice versa. D_{11} attenuates reverse polarity voltages from the base to emitter of T_{17}, whereas R_{60} is needed to insure proper cut-off (and thus stability) of T_{17}. D_9 also is a back-swing protecting diode. R_{58} was found necessary to provide adequate damping and eliminate ringing.

The delay lines for the 10- and 20-μsec pulses and a blocking oscillator for the 5-μsec clock pulses were chosen as follows. It was desired to have extremely stable width pulses for start and stop time markers. Constant width clock pulses were much less necessary, since clock pulses serve only as convenient ground-station telemetry tracking signals and accelerometer recycle time reference markers. Pulse forming by delay lines involves no active elements in pulse-width determination and thus reliable constant width pulses can be much more easily attained. Hence the 10- and 20-μsec pulses were formed in this manner. On the other hand, pulse forming with blocking oscillators is simpler to design, and much less expensive. Since the characteristics of blocking oscillator pulses were entirely satisfactory for the clock-pulse application, these pulses were formed in this manner.

5.4 ACCELEROMETER DRIVE

The accelerometer drive circuit is the circuit used to energize the accelerometer coils used in recentering the bobbin. It consists of T_{21} for drive-signal amplification and T_{22} as the high current switch. The 150-millisecond reset pulse is delivered to the base of T_{21} through R_{62}. In flight the switch FS_1 is closed so that the emitter of T_{21} is tied directly to the base of T_{22}. T_{21} is normally cut-off, so that no current flows into the base of T_{22}. The purpose of R_{65} is to keep the emitter of T_{21} from floating when FS_1 is open. The purpose of R_{64} is to keep the base of T_{22} from floating when FS_1 is open. With FS_1 closed the R_{64}-R_{65} parallel combination prevents I_{EO} of T_{21} from flowing in the base of T_{22} and becoming amplified. R_{63} is simply a current-limit-

ing resistor to keep from over-driving T_{21}. The 150-msec current pulse from T_{21} is amplified again in T_{22}, and flows through the accelerometer coils (which are in parallel with D_{12}) causing the accelerometer fingers to function. The purpose of D_{12} is to eliminate any inductive pulses which could harm T_{22}. The only critical portion of this circuit is the parallel combination of R_{64} and R_{65}. This value must be large enough so that most of the T_{21} emitter saturation current flows into the base of T_{22}, but must be small enough so that the I_{EO} in T_{21} cannot raise the base voltage of T_{22} high enough to cause T_{22} to begin conduction. The value of this resistance is, then, dependent upon the magnitude of I_{EO} of T_{21} and the emitter-to-base cut-off voltage of T_{22}. The design values shown have been adequate for all combinations of 2N456A transistors used for T_{22} and 2N1184 transistors used for T_{21}.

5.5 PULL-OFF PLUG

This assembly provides for operating the sphere system with an external power source, and for monitoring the sphere power supply voltage, prior to flight. This is done so that the batteries in the sphere do not have to supply power while the system is operating during the rocket firing count-down. It also allows a continuous pre-flight check on the sphere battery voltage. This plug is pulled out a few seconds before firing and power is then supplied by the internal batteries. An extra benefit of this scheme is that it actually allows observation of proper circuit functioning during the time that the pull-off plug is engaged—thereby giving an additional, last-minute check on the proper functioning of the system.

The plug is a pressurized 4-terminal plug, two terminals for providing the load-floating current, and two for monitoring the battery voltage. These are shown on the circuit diagram. The components D_{21} and R_{76} are needed for protection against accidental pull-off plug pin shorts during or after the plug is pulled from the sphere prior to rocket takeoff.

5.6 POWER SUPPLIES

All power supplies used in the system are derived from the bank of 6 HR-1 silvercells in series (B_1 through B_6). Each of these cells individually maintains a nominal voltage of 1.5 volts across its terminals—making 9 volts for the series bank. This 9 volts is used directly for the -9 volt supplies indicated throughout the entire circuit diagram. The regulated 6-volt supply is obtained across D_{20} and filter capacitor C_{32}. The diode D_{20} is a 6.0-volt zener diode. The dynamic impedance of D_{20} (IN752) is about 7 ohms; thus regulation is not perfect because the series dropping resistor R_{75} is only 22 ohms. However, it has proven very adequate for this application.

The 85-volt modulator supply voltage is obtained from the 9-volt silvercell supply by means of a d-c to d-c converter. This circuitry is shown on

the circuit diagram with the label "Modulator Supply." The converter circuit, employing transistors T_{24} and T_{25}, is of conventional design. The circuitry following the power supply filter consists of dropping resistor R_{74}, a smoothing capacitor C_{31} and an 85-volt zener diode D_{19}. The principal purpose of the zener diode is not for regulating purposes, but rather to insure that the nominal 85-volt supply voltage never substantially exceeds 85 volts and thus prevents possible damage to transistors T_{18}, T_{19}, and T_{20} in the modulating unit. The converter transformer TR_3 was designed for operation with an input voltage of 28 volts. Since it is used here with an input voltage of 9 volts, its design output voltage is also reduced by 9/28 to approximately 85 volts.

5.7 SWITCHING

There are two mechanical switches in the complete sphere assembly. One is the simple "open or closed" switch (FS_1) used to keep the accelerometer inactive until the sphere is ejected from the nose cone, and herein referred to as the "fly switch." The other mechanical switch is a clarostat three-pole, four-position function switch.

The fly switch is a special pressurized subminiature microswitch, used in the "open when depressed—closed when released" configuration. It is incorporated in the accelerometer drive circuit as shown between the emitter of T_{21} and the base of T_{22}, and actuated by a spring-loaded plunger that, when released, is flush with the smooth outside surface of the sphere. To depress the switch mechanism, the plunger is pushed inwards about an eighth of an inch. As the sphere is being installed in the rocket nose cone, a 1/8-in. steel ball is inserted into the hollow in the sphere caused by depressing the plunger, and bears against an assembly in the nose cone, thereby keeping the fly switch plunger depressed and the switch open. Upon ejection of the sphere from the nose cone the assembly retaining the steel ball is no longer present, and the spring forces the plunger back outwards, thus closing the fly switch. The purpose of the fly switch is, of course, to keep the accelerometer inoperative during the high accelerations of rocket take-off, second-stage ignition, and high-velocity drag forces so as to avoid damage to the pick-up finger bearings. Normal operation of the entire system commences upon ejection of the sphere from the nose cone and the closure of the fly switch FS_1. Until closures of FS_1 the logic circuitry is recycling every 2.5 seconds due to the action of the over-ride circuit.

The function switch is used for turning power to the circuitry on and off, and to set up certain testing conditions. The functions performed by the function switch, as shown on the circuit diagram, are:

Position 1	Off
Position 2	Balance
Position 3	Test
Position 4	Fly

Position 1 simply disconnects all power from the circuits. Position 2 energizes only the accelerometer pick up coils by placing them directly across the 9-volt supply. In this position it is possible to balance the sphere with the accelerometer bobbin centered. Position 3 puts the entire system in normal functioning configuration with the single exception that the fly switch is bypassed with a short circuit. This allows test cycling of the accelerometer with the sphere in the nose cone. Position 4 engages the entire system in normal functioning configuration and ready for flight. The operation of all circuits under this configuration is as described in detail above.

It will be noticed that one of the poles, A or B, is apparently redundant in that the pole arms of these two both go to the positive side of the 9-volt supply. The purpose of pole B is to energize the converter circuitry whereas pole A switches power to all other parts of the system. It was found that, if this separation was not employed, interfering pulses were present on the supply lines. These pulses were found to come from the (relatively) high-current, high-speed switching action of transistors T_{24} and T_{25} in the converter. The best solution to this was found to be the use of separate supply lines (both positive and negative) for the converter and for the other circuitry. This makes necessary the use of both A and B poles as shown. Pole B was given the additional task of connecting the accelerometer coils across the 9-volt supply. Pole C connects the fly switch properly in all positions. It will also be noticed that the "ground" side of the circuitry (the positive side of the battery) has been on-off-switched rather than the "hot" side (negative side of the 9-volt supply). This was done to eliminate the need for a fourth pole when using the function switch in position 2, and creates no system problems.

5.8 COMPONENTS (See Table IV)

5.8.1. Transistors.—Most of the circuitry is logic switching circuitry using d-c level logic with pulse triggering. For this application transistors were needed that had the following characteristics:

(1) high switch speeds
(2) high current capabilities
(3) large h_{FE} for both large and small collector currents
(4) 8 to 10 volts rating for reverse base to emitter bias (min)
(5) economical
(6) either NPN or PNP
(7) either silicon or germanium

Both germanium and silicon transistors (and NPN and PNP) were available to meet the first three specifications. However, to meet specifications (4) and (5), we had to resort to germanium. After an extensive search and testing of various transistor types, PNP type 2N414 was chosen as the main transistor

TABLE IV*

COMPONENT FUNCTION

Transistor and Diode	Application	Configuration
T_1	Emitter follower	Quiescent Biasing. Emitter = -5 volts
T_2	Amplifier-switch	Cut-off; saturated when contact pulse occurs
$T_3(T_4)$	Bistable Multivibrator	Cut-off (saturated); saturates (cuts off) when triggered by contact pulse
$T_5(T_6)$	Astable Multivibrator	Saturated (cut-off) during most of 350 ms cycle. Cut off (saturated) during 10 ms clock pulse
$T_7(T_8)$	Monostable Multivibrator	Cut-off (saturated); saturated (cut-off) during 150 ms recycling interval
$T_9(T_{10})$	Monostable Multivibrator	Saturated (cut off)—(quasi stable state—2.5 sec)
$T_{11}(T_{12})$	Monostable Multivibrator	Cut off (saturated)→[saturates (cuts off) for 2.5 ms at bobbin release]
$T_{13}(T_{14})$	Amplifier switch	Cut off; saturates for start (stop) pulse
$T_{15}(T_{16})$	Switch	Cut off; saturated during start (stop) pulse
T_{17}	Blocking Oscillator	Cut off; saturated during 5 μsec clock pulse
$T_{18}(T_{19},T_{20})$	Power Switch	Cut off; saturated during 5 μsec (start and stop) clock pulse(s)
$T_{21}(T_{22})$	Amplifier switch (power switch)	Cut off—saturated during 150 ms recycling
T_{23}	Oscillator	Class A biased
$T_{24}(T_{25})$	Converter Oscillator	Alternately saturated and cut off
$D_1(D_2)$	"AND" Logic	Normally conducting
D_3,D_4,D_5	"Power Supplies"	Always conducting at least 6 ma
D_6,D_7	"OR" Logic	Normally nonconducting
D_8, D_9, D_{10}, D_{11}, D_{12}	Reverse Voltage-Protection	Normally nonconducting
$D_{13}(D_{20})$	Zener diode	7.0 (6.0) volt regulated supply
D_{14}	Rectifier	Low forward voltage drop
D_{15}, D_{16}, D_{17}, D_{18}	Bridge Rectifier	High voltage—high current
D_{19}	Zener Diode	Keeps supply from exceeding 85 volts
D_{21}	Reverse Current Switch	Protects against accidental shorting of pull-off terminals

*The "application" column the type of circuit in which the element is used. The "configuration" column comments on operation of the element during the interval of time that the bobbin is in the process of freely falling toward the cavity wall unless specified.

element for the logic circuitry. A 2N1090 was chosen as the NPN counterpart when complementary circuitry was required.

In several places other transistor types were used when special applications or characteristics were required. The 2N1381 used for T_1 has a higher h_{FE} in the collector current region over which it operates than does the 2N-414 or 2N1090, and is thus better for the input stage application. The 2N1-231 used for T_8 is another special-purpose transistor. It is a PNP silicon switching transistor with a reasonably high h_{FE}. It exhibits greater temperature stability than is possible with germanium transistors. The 2N370 used for T_{23} is a high-frequency transistor designed specifically for HF oscillator applications. The characteristics of the 2N1184 used for T_{24} and T_{25} (and also for T_{21}) are very similar to those of the 2N414 except that it has a considerably higher current and power rating. The 2N456A used for T_{22} is a high current switching transistor. The 3 amperes flowing through the accelerometer coils all pass through T_{22}, thus necessitating such a transistor. The 2N1715, used for T_{18}, T_{19}, and T_{20}, is perhaps the most special of all the transistors used. For this application a transistor was needed that had:

(1) a high emitter to collector voltage rating (90 volts/min)
(2) a high collector current rating (1.0 amp)
(3) high switching speed, and low storage time (less than 1.0μsec)

Most transistors failed to qualify on at least one of the above specifications. The 2N1715, with a voltage rating of 100 volts, a current rating of 1.0 amp, and switching speeds of less than 1-μsec, proved to be ideal for this application. Other transistors were discovered that would have been satisfactory, but all had lower effective values of h_{FE}, and thus would not saturate as quickly as the 2N1715. Moreover, storage time in the 2N1715 was less than any other usable type. All the transistor types suitable for application as T_{18}, T_{19}, and T_{20} were NPN silicon transistors, including the 2N1715.

During all experience with this design, selected units were not required and no transistor failures occurred using the configurations and components as shown in the circuit diagram.

5.8.2. Diodes.—The diodes in the system are of four types:

(1) Logic and "circuit" diodes;
(2) Current and voltage surge protecting elements;
(3) Zener (voltage regulating) diodes;
(4) Rectifying diodes.

D_{14} is a 1N100A, and was chosen for its low forward resistance characteristic. It is a germanium diode and thus maintains a much smaller forward conducting voltage across it than would a typical silicon diode. All other diodes

in the system are silicon diodes. D_{15}, D_{16}, D_{17}, and D_{18} were chosen specifically for their high reverse voltage and high forward current characteristics for the bridge rectifier. The zener diodes D_{13}, D_{19}, and D_{20} are 7.0 volts, 85 volts, and 6.0 volts, respectively, and are used for voltage regulating purposes. The rest of the diodes in the system are all standard silicon diodes. Those making up (2) above are all the same type (1N2071). This seems to be an extremely good diode, as it can withstand several hundred volts in the reverse direction, and momentary surge currents of several amperes in the forward direction. The rest of the diode applications in the system [comprising (1) above] include a variety of configurations. However, the characteristics needed in each case did not differ greatly, and it was decided to choose, from the multitude of available diodes, one type that would be satisfactory for use in any of the logic circuitry applications. The type chosen was the 1N482A, and it has proven very satisfactory. D_3, D_4, and D_5 are used as miniature "power supplies" (as described previously) whereas D_1, D_2, D_6, D_7 are used for standard "AND" and "OR" logic. D_{11} is used as a nonlinear resistance device in the blocking oscillator circuit.

As with the transistors, not a single diode failure has been experienced under normal operation of this design.

5.8.3. **Capacitors.**—The following Types of capacitors are employed:

(1) tantalum electrolytic;
(2) ceramic;
(3) mica;
(4) aluminum electrolytic.

Only C_{30} and C_{31} are aluminum electrolytic. The higher voltage requirement, along with high capacitance, without need for extremely low leakage, indicated standard electrolytics for these two. Mica capacitors are used only for the low-capacitance, high-precision capacitances in the contact detector circuitry. Tantalum electrolytics and ceramic capacitors are used widely throughout the system. All the smaller-value capacitances (less than one microfarad) are ceramics. All the low-voltage capacitance applications employ the new low-voltage ceramics, as a space-saving feature. All capacitances higher than one microfarad (and marked with polarity signs), except C_{30} and C_{31}, are low-voltage Texas Instrument tantalum capacitors. In particular C_4 and C_5 are TI tantalums and exhibit the "positive temperature coefficient" for aiding in temperature compensation of the clock circuit.

5.8.4. Pulse Transformers.—The pulse transformer used for PT_1 and PT_2 are the Technitrol (series TE) pulse transformers. The Technitrol series AMB (special small-scale transistor application pulse transformers) were tested and found unsatisfactory due to a systematic internal mechanical failure. The types used in this system (G13WA and 03QA) are heavier-duty types than the AMB

series and have proven very satisfactory. The G13WA(PT_1) is a 22-millihenry primary inductance, three winding transformer, with a 3 to 3 to 1 turns ratio. The first and last windings have been used in series, with the middle winding being used as the secondary. PT_2 (the 03QA) is a 1-millihenry primary inductance transformer, also with a 3 to 3 to 1 turns ratio winding pattern. The low turns number winding is used in the emitter circuit of the blocking oscillator. PT_3 is a 2 winding type D5315U4A custom built pulse transformer made by the Fischer Company. It has a 1 to 5 primary to secondary turns ratio. The transmitter presents a secondary load of about 2200 ohms, reflected into the primary as about 80 ohms.

TR_3 is a commercially available specialized transformer for d-c to d-c converter applications. It is made by the Triad Co. (TY-88) and is designed to operate on an input of 28 volts.

5.8.5. Delay Lines.—The delay lines PFN_1 and PRN_2 were designed and built in this laboratory and are 10-section, lumped-constant, 5 and 10-μsec, respectively, open-circuited delay lines. The circuit diagram for each is shown in Fig. 30. For each line there are 10 identical C's in the configuration as shown. In the case of PFN_1 (5-μsec delay line, 10-μsec pulse-forming network) the capacitors are 0.005 microfarad, and the inductors are 50 microhenries each. For PFN_2 (10-μsec delay line, 20-μsec pulse-forming network) the capacitors are 0.01 microfarad, and the inductors are 100 microhenries.

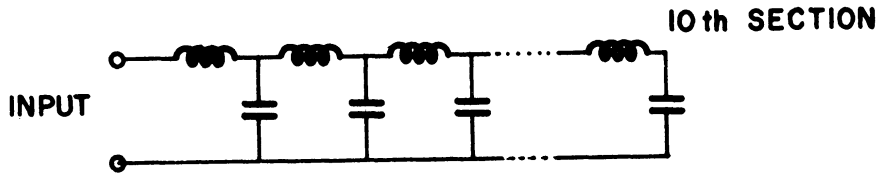

Fig. 30. Ten-section delay line.

The capacitors are Centralab type DM low-voltage ceramics and the individual inductances were wound on General Ceramics type CF-102Q1 toroids. The 50-microhenry toroids required approximately 32 turns of No. 33 enameled wire and the 100-microhenry toroids required approximately 48 turns of No. 33 wire.

The characteristic impedance of each line is 100 ohms. The values of L and C were determined by the following criterion.

The approximate formulas for lumped constant delay lines are:

$$T = n\sqrt{LC}$$

$$Z_o = \sqrt{\frac{L}{C}}$$

where

T = the delay time

Z_o = characteristic impedance

n = number of sections

L and C are as in Fig. 30 above

From this:

$$L = \frac{TZ_o}{n}$$

and

$$C = \frac{T}{nZ_o}$$

Thus, given the values of T, Z_o, and n, the values for L and C were easily determined. Of course, T was known from system specifications, Z_o was quickly established from optimum circuit considerations, and the value of n was established by experiment. All these, in turn, immediately established the values of C and L.

6. ACKNOWLEDGMENT

This work was sponsored by Geophysics Research Directorate, Office of Aerospace Research, U. S. Air Force whose cooperation and support is gratefully acknowledged.

7. REFERENCES

1. Bartman, F. L., Chaney, L. W., Jones, L. M., and Liu, V. C., "Upper-Air Density and Temperature by the Falling Sphere Method," J. Appl. Phys., 27, 706-712 (1956).

2. Jones, L. M., "Transit-Time Accelerometer," Rev. Sci. Instr., 27, 374-377 (1956).

3. Jones, L. M., and Bartman, F. L., A Simplified Falling-Sphere Method for Upper-Air Density, Univ. of Mich. Eng Res. Inst. Rept. 2215-10-T, Ann Arbor, 1956.

4. Peterson, J. W., Analytical Study of the Falling-Sphere Experiment for Upper-Air Density Measurements, Univ. of Mich. Eng. Res. Inst. Rept. 2533-2-T, Ann Arbor, 1956.

5. Jones, L. M., Fischbach, F. F., and Peterson, J. W., "Seasonal and Latitude Variations in Upper Air Density," Natl. Acad. Sci., IGY Rocket Rept. Series, 1, 47-57 (1958).

6. Peterson, J. W., Schaefer, E. J., and Schulte, H. F., A Simplified Falling-Sphere Method for Upper-Air Density, Part II. Density and Temperature Results from Eight Flights, Univ. of Mich. Res. Inst. Rept. 2215-19-F, Ann Arbor, 1959.

7. Jones, L. M., Peterson, J. W., Schaefer, E. J., and Schulte, H. F., "Upper-Air Densities and Temperatures from Eight IGY Rocket Flights by the Falling-Sphere Method," Natl. Acad. Sci., IGY Rocket Rept. Series, 5 (1959).

8. Jones, L. M., Peterson, J. W., Schaefer, E. J., and Schulte, H. F., "Upper-Air Density and Temperature: Some Variations and an Abrupt Warming in the Mesosphere," J. Geo. Res., 64, 2331-2340 (1959).

9. Jones, L. M., and Peterson, J. W., Upper-Air Densities and Temperatures Measured by the Falling Sphere Method, 1961 Review, Univ. of Mich., ORA Rpt. 03558-5-T, Ann Arbor, 1961.